JOC The Journal of Organic Chemistry

Article

pubs.acs.org/joc

Synthesis and Photophysical Properties of Biaryl-Substituted Nucleos(t)ides. Polymerase Synthesis of DNA Probes Bearing Solvatochromic and pH-Sensitive Dual Fluorescent and ^{19}F NMR Labels

Jan Riedl, Radek Pohl, Lubomír Rulíšek, and Michal Hocek*

Institute of Organic Chemistry and Biochemistry, Academy of Sciences of the Czech Republic, Gilead Sciences & IOCB Research Center, Flemingovo nam. 2, CZ-16610 Prague 6, Czech Republic

Supporting Information

ABSTRACT: The design of four new fluorinated biaryl fluorescent labels and their attachment to nucleosides and nucleoside triphosphates (dNTPs) by the aqueous cross-coupling reactions of biarylboronates is reported. The modified dNTPs were good substrates for KOD XL polymerase and were enzymatically incorporated into DNA probes. The photophysical properties of the biaryl-modified nucleosides, dNTPs, and DNA were studied systematically. The different substitution pattern of the biaryls was used for tuning of emission maxima in the broad range of 366−565 nm. Using methods of computational chemistry the emission maxima were reproduced with a satisfactory degree of accuracy, and it was shown that the large solvatochromic shifts observed for the studied probes are proportional to the differences in dipole moments of the ground (S_0) and excited (S_1) states that add on top of smaller shifts predicted already for these systems *in vacuo*. Thus, we present a set of compounds that may serve as multipurpose base-discriminating fluorophores for sensing of hairpins, deletions, and mismatches by the change of emission maxima and intensities of fluorescence and that can be also conviently studied by ^{19}F NMR spectroscopy. In addition, aminobenzoxazolyl-fluorophenyl-labeled nucleotides and DNA also exert dual pH-sensitive and solvatochromic fluorescence, which may imply diverse applications.

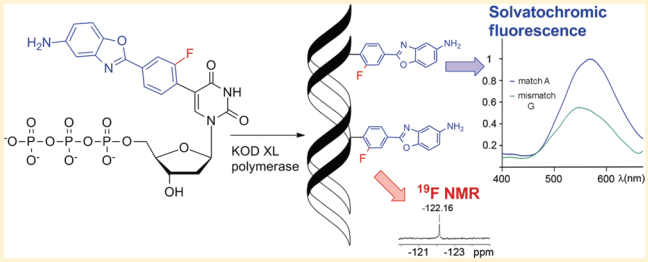

INTRODUCTION

Fluorescence labeling of biomolecules[1] and fluorescence analytical methods have recently become one of the most frequently used techniques in chemical biology. Nucleic acids bearing fluorescent labels are widely used probes in molecular biology for genomic sequencing[2] or for the detection of infections or genetic diseases by molecular beacons.[3] The fluorophores can be attached to nucleic acids in several ways: to phosphate or sugar moiety or to nucleobase via a conjugate or nonconjugate linker, or a fluorophore can even replace a nucleobase. The fluorophores attached via longer nonconjugate aliphatic linkers are generally used for the detection in sequencing[2] or FRET techniques[3] and are favorable for decreasing the steric hindrance in enzymatic reactions and during DNA hybridization. The intrinsically fluorescent nucleoside analogues (IFN), where a fluorophore is linked directly[4] or via conjugate tether[5] or replacing a nucleobase either by a fused analogue[6] or even by a structurally unrelated molecule,[7] typically respond well to hybridization (base-discriminating fluorophores, BDF) and formation of secondary structures. Even the use of a nonconjugate but short propargylamide linker for attachment of fluorophores (e.g., pyrene) resulted in the specific response of the fluorescence to single nucleotide polymorphism (SNP).[8]

Fluorescent pH sensors are an important class of compounds mostly applied in the development of novel functional materials. Very interesting and useful fluorescent pH sensors in cell and molecular biology are dual fluorescent pH sensors that change the emission maxima in the physiological range of pH.[9] Particularly interesting fluorophores are the dual fluorescent mutants of green fluorescent protein, which can be directly expressed in the cell.[10] Several phenol-substituted nucleosides exerted fluorescent pH-sensing properties.[11] Dual fluorophores connected to nucleic acids may be attractive for measurement and visualization of microenvironments with different pH values associated with various biological processes. This may also indicate difference between tumor and normal tissues.

NMR spectroscopy plays also an important role in the structural studies of nucleic acids. Particularly, the measurements of ^{19}F nuclei were shown to be advantageous owing to its low abundance compared to ^{1}H (typically, an artificial fluorinated substituent is introduced site-specifically). Their sensitivity and high range of chemical shifts reflect better the structure and hybridization in 1D experiments. ^{19}F NMR

Received: November 9, 2011
Published: December 12, 2011

spectroscopy was successfully implemented for studies of structural motives, ligand binding and hybridization of diverse fluorine-labeled nucleic acids.[12]

Apart from the chemical synthesis, base-modified DNA can be prepared enzymatically by polymerase incorporations of the base-modified deoxyribonucleoside triphosphates (dNTPs).[13] Particularly efficient is the single-step synthesis of modified dNTPs by aqueous cross-coupling reactions followed by the polymerase incorporation. The polymerase incorporation of modified dNTPs has been extensively used for fluorescence,[14] redox,[15] and spin[16] labeling on DNA. Also, RNA polymerase incorporation of fluorescent ribonucleoside triphosphates was used for the construction of fluorescent RNA.[17]

The aim of this work is the construction of functionalized DNA bearing novel versatile multipurpose biaryl labels capable of base-discriminating, solvatochromic and/or pH-sensitive fluorescence and ^{19}F NMR detection. Four different types of biaryl groups have been designed: 4-methoxybiphenyl (**BIF**), 2-phenylbenzofuryl (**BFU**), 2-phenylbenzoxazole (**BOX**), and 2-phenyl-5-aminobenzoxazole (**ABOX**) directly bound at the 5-position of pyrimidines or at 7-position of 7-deazapurines with a fluorine substituent in the *ortho* position. The study includes the synthesis of nucleosides and dNTPs, polymerase incorporations, photophysical properties of nucleosides (including pH and solvent effects) studied both experimentally and computationally, different secondary structures of DNA, and the ^{19}F NMR spectroscopy.

RESULTS AND DISCUSSION

Synthesis. The attachment of the above-mentioned biaryls to nucleosides and dNTPs was planned to be realized by the Suzuki–Miyaura cross-couplings of halogenated nucleos(t)ides with the corresponding biarylboronates. Therefore, the first task was the synthesis of pinacol esters of biarylboronates via the Suzuki coupling of the corresponding brominated biaryls (**1a–1d**) with bis(pinacolato)diboron. 4-Methoxyphenyl- (**1a**) and benzofuryl- (**1b**) derivatives were prepared in good yields by the Suzuki coupling of 1-bromo-2-fluoro-4-iodobenzene with the corresponding arylboronic acids (Scheme 1) in the presence of $Pd(PPh)_3Cl_2$ and K_2CO_3 in DMF. The benzoxazole (**1c**) and aminobenzoxazole (**1d**) derivatives were efficiently prepared by cyclization reaction of aminophenols with 4-bromo-3-fluorobenzoic acid in the presence of polyphosphoric acid (Scheme 1). The biaryl bromides (**1a–1d**) were converted to the desired pinacol-boronates **2a–2d** (59–74% yields) by the cross-coupling with B_2Pin_2 catalyzed by $PdCl_2$(dppf) in presence of potassium acetate in dry dioxane (Scheme 1).

The aqueous-phase Suzuki–Miyaura cross-coupling reactions of boronates **2a–d** with 7-iodo-7-deaza-2′-deoxyadenosine (**dA^{I}**) or 5-iodo-2′-deoxyuridine (**dU^{I}**) in the presence of the $Pd(OAc)_2$/TPPTS catalytic system and Cs_2CO_3 in H_2O/CH_3CN (Scheme 2, Table 1) gave the desired biaryl-substituted nucleosides **dN^{R}** in moderate to good yields (44–71%). Analogously, the halogenated dNTPs (**dA^{I}TP** and **dU^{I}TP**) reacted with the boronates **2a–d** to give directly the biaryl-dNTPs (**dN^{R}TP**) in yields of 17–28%, somewhat lowered due to the hydrolysis of the triphosphate during the coupling reaction.

Incorporation of the Modified dN^{R}TPs by DNA Polymerase. The biaryl-modified **dN^{R}TPs** were tested in primer extension (PEX; for primers and templates, see Table 2) incorporations using several DNA polymerases (KOD XL, Vent (exo-), Phusion, Therminator, 9°N DNA polymerase). The best results were obtained using KOD XL DNA polymerase, which was able to incorporate all the **dN^{R}TPs** smoothly to achieve the full length products containing 4 modified nucleotides (Figure 1). In comparison, Vent(exo-) did not give full-length products (Figure S7 in Supporting Information). The PEX products show slightly different mobilities in polyacrylamide gel electrophoresis (PAGE), but a set of representative samples of products containing **dA^{BFU}**, **dA^{BOX}**, and **dU^{BOX}** modifications was characterized by MALDI-TOF analysis (see Experimental Section) as the correct full-length products. The MALDI analysis also excluded any potential misincorporation of natural dNTPs. The increased mobilities of some oligonucleotides may be caused by more packed DNA conformations due to the hydrophobic interactions of the biaryl-modifications. The PEX products of incorporation of modified **dU^{R}** in analytical scale contained a one-nucleotide shorter impurity (Figure 1, lanes 9–12), but in preparative scale, the PEX gave clean full-length products (Figure S8 in Supporting Information).

Scheme 1. Synthesis of Biaryl Pinacolatoboronates[a]

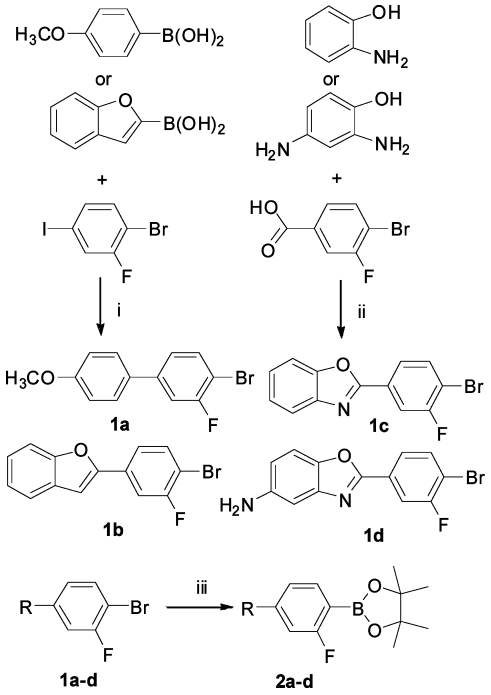

[a]Reagents and conditions: (i) $Pd(PPh_3)_2Cl_2$, K_2CO_3, DMF, 80 °C, 5 h, yields **1a** (74%), **1b** (85%); (ii) polyphosphoric acid, 170 °C, 16 h; yields **1c** (89%), **1d** (94%); (iii) **1a–1d**, B_2Pin_2, $PdCl_2$(dppf), KOAc, dioxane, 80 °C, 1 h, yields **2a** (62%), **2b** (59%), **2c** (65%), **2d** (74%) respectively.

Thermal Denaturation Study. For comparison and determination of the influence of modifications on the DNA hybridization, thermal denaturation studies were performed for the oligonucleotides containing single and multiple incorporations. All modified oligonucleotides showed destabilizing effect characterized by 2–3 °C decrease of melting temperature per modified nucleobase (Table 3). The stability of single-functionalized duplexes is only slightly affected (2–3 °C), while duplexes containing four modifications show proportional destabilization (up to 12 °C). Since these fluorophores are assumed to be used as single-positioned labels in modified oligodeoxyribonucleotides, their destabilization effect is acceptable.

dx.doi.org/10.1021/jo202321g | J. Org. Chem. 2012, 77, 1026–1044

Scheme 2. Synthesis of Modified Nucleosides and Nucleoside Triphosphates[a]

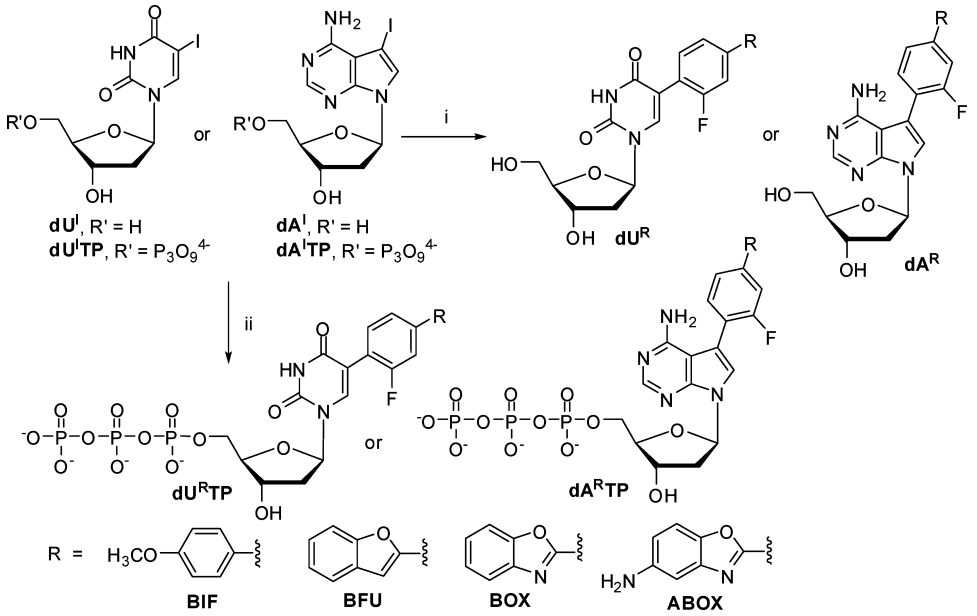

[a]Reagents and conditions: (i) **2a-2d**, $Pd(OAc)_2$, TPPTS, Cs_2CO_3, H_2O/CH_3CN (2:1), 80 °C, 2 h; (ii) **2a-2d**, $Pd(OAc)_2$, TPPTS, Cs_2CO_3, H_2O/CH_3CN (2:1), 90 °C, 0.75 h.

Table 1. Preparation of Biaryl Modified Nucleosides (dN^R) and dNTPs (dN^RTP)

entry	boronate	dN^I	dN^R	yield (%)	dN^ITP	dN^RTP	yield (%)
1	**2a**	dA^I	dA^{BIF}	61	dA^ITP	$dA^{BIF}TP$	22
2	**2b**	dA^I	dA^{BFU}	69	dA^ITP	$dA^{BFU}TP$	28
3	**2c**	dA^I	dA^{BOX}	57	dA^ITP	$dA^{BOX}TP$	23
4	**2d**	dA^I	dA^{ABOX}	44	dA^ITP	$dA^{ABOX}TP$	26
5	**2a**	dU^I	dU^{BIF}	65	dU^ITP	$dU^{BIF}TP$	21
6	**2b**	dU^I	dU^{BFU}	59	dU^ITP	$dU^{BFU}TP$	17
7	**2c**	dU^I	dU^{BOX}	71	dU^ITP	$dU^{BOX}TP$	20
8	**2d**	dU^I	dU^{ABOX}	61	dU^ITP	$dU^{ABOX}TP$	25

Photophysical Properties of the Modified Nucleosides. The absorption and fluorescence emission spectra of all biaryl-modified nucleosides dN^R were measured in methanol (Figure 2, Table 4). The emission maxima as well as the intensities differ depending on the nucleobase and on the biaryl substitution pattern. dA^{BIF} (λ_{em} = 366, 386 nm), dA^{BFU} (λ_{em} = 409 nm), dA^{BOX} (λ_{em} = 475 nm) exhibit red-shifted emission spectra compared to free biaryl fluorophores (the corresponding boronates **2a**−**2d**) emitting almost at the same emission maximum regardless of the structural changes (λ_{em} = 348−355 nm) (see Figure S10 in Supporting Information) apparently caused by conjugation with adenosine. Replacement of benzofurane (dA^{BFU}) by benzoxazole (dA^{BOX}) causes another significant red shift of the emission (λ_{em} = 475 nm). The fluorescence intensities of dA^R nucleosides decrease with longer-wavelength emission maxima. In contrast to dA^R, the uridine portion of fluorophores tended to decrease intensity of the emission (dU^{BIF} is nonfluorescent) and change the fluorescence properties of dU^{BFU} and dU^{BOX}. The dU^{BOX} shows a more intense fluorescence at slightly shorter wavelength than dU^{BFU}, whereas both are still slightly red-shifted by conjugation with uridine compared to free fluorophores. The addition of an electron-donating amino group in dA^{ABOX} further significantly red-shifted the emission maximum up to 535 nm (yellow fluorescence). On the other hand, the dU^{ABOX} shows a dual fluorescence (λ_{em} = 422, 538 nm; Figure 2b, Table 4) originating from the presence of a small amount of highly emissive protonated form of dU^{ABOX} (vide infra).

Solvatochromic Fluorescence of ABOX Nucleosides. **ABOX** boronate (**2d**) itself (Figure S11 in Supporting Information) and both dN^{ABOX} nucleosides exerted bathochromic (red-shifted) solvatochromic effect. The intensity of fluorescence strongly decreases while emission maxima are red-shifted with increasing solvent polarity. The emission maxima change from 480 nm in dioxane to 565 nm in water for dA^{ABOX} while the intensity decreases 70-fold (Figure 3). dU^{ABOX} exerted similar solvatochromic effects, but the fluorescence spectra showed additional violet emission (λ_{em} = 422 nm) in methanol and (λ_{em} = 406 nm) in water originating from the acidic form of dU^{ABOX} also observable under neutral conditions (vide infra). For quantification of the solvatochromic effects, see Figure S9 in Supporting Information, and for UV spectra see Figure S13 in Supporting Information.

Computional Study of dA^R Photophysical Properties. In order to explain the observed photophysical properties of the studied compounds, quantum chemical calculations of the absorption and emission spectra have been carried out, both in the gas-phase and in solvent (using the implicit solvation model) for three simplified model compounds, 9-methyl-7-deazaadenine derivatives MeA^{ABOX}, MeA^{BOX}, and MeA^{BFU}. We presume

dx.doi.org/10.1021/jo202321g | J. Org. Chem. 2012, 77, 1026−1044

Table 2. Oligo-2′-deoxyribonucleotides Used or Synthesized in This Study

oligonucleotide	oligodeoxyribonucleotide sequence (5′−3′)
Prim1[a]	5′-d(CATGGGCGGCATGGG)
Prim2[a]	5′-d(GGGTGGGTGGGTGGCTTTTGT)
Prim3[a]	5′-d(GGGTGGGTGGGTGGTTGT)
ON1	5′-d(CATGGGCGGCATGGGA^{R}GGG)
ON2	5′-d(CATGGGCGGCATGGGU^{R}GGG)
ON3	5′-d(GGGTGGGTGGGTGGCTTTTGTU^{R}AAAAAGGGG)
ON4[a]	5′-d(CCCCTTTTTAACAAAAGCCACCCACCCACCC)
ON4(bio)[a]	(bio) 5′-d(CCCCTTTTTAACAAAAGCCACCCACCCACCC)
ON5	5′-d(GGGTGGGTGGGTGGTTGTU^{R}AAGGG)
ON6	5′-d(CATGGGCGGCATGGGCAGCU^{R}GGACGACGAA)
ON7[a]	5′-d(TTCGTCGTCCAGCTGCCCATGCCGCCCATG)
ON7(bio)[a]	(bio) 5′-d(TTCGTCGTCCAGCTGCCCATGCCGCCCATG)
ON8[a]	5′-d(TTCGTCGTCCACTGCCCATGCCGCCCATG)
ON9[a]	5′-d(TTCGTCGTCCGCTGCCCATGCCGCCCATG)
ON10[a]	5′-d(TTCGTCGTCCCGCTGCCCATGCCGCCCATG)
ON11[a]	5′-d(TTCGTCGTCCTGCTGCCCATGCCGCCCATG)
ON12[a]	5′-d(TTCGTCGTCCGGCTGCCCATGCCGCCCATG)
ON13[a]	5′-d(CCCTCCCATGCCGCCCATG)
ON13(bio)[a]	(bio) 5′-d(CCCTCCCATGCCGCCCATG)
ON14[a]	5′-d(CCCGCCCATGCCGCCCATG)
ON15[a]	5′-d(CCCACCCATGCCGCCCATG)
ON15(bio)[a]	(bio) 5′-d(CCCACCCATGCCGCCCATG)
ON16[a]	5′-d(CCCCCCCATGCCGCCCATG)
ON17 (U^{R})	5′-d(CATGGGCGGCATGGGACU^{R}GAGCU^{R}CAU^{R}GCU^{R}AG)
ON18[a]	5′-d(CTAGCATGAGCTCAGTCCCATGCCGCCCATG)
ON18(bio)[a]	(bio) 5′-d(CTAGCATGAGCTCAGTCCCATGCCGCCCATG)
ON19[a]	5′-d(CCCTTAACAACCACCCACCCACCC)
ON19(bio)[a]	(bio) 5′-d(CCCTTAACAACCACCCACCCACCC)

[a]Purchased oligonucleotide, (bio) = 5′-biotinylated.

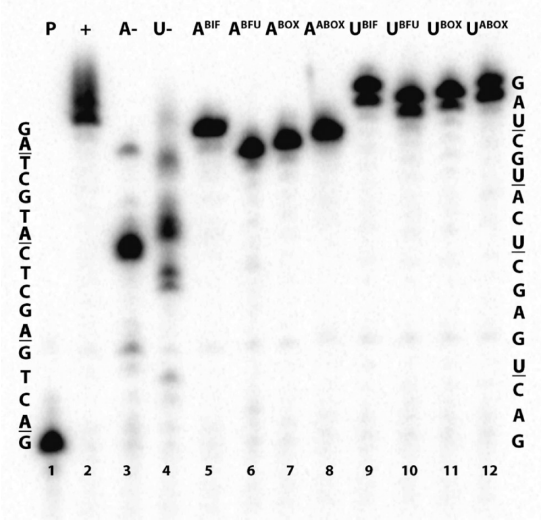

Figure 1. Multiple incorporations of **dN^{R}TP** by KOD XL DNA polymerase. The gel shows eight PEX experiments for the study of **dN^{R}TP** incorporation denoted **A^{R}** or **U^{R}**. Experiments are supplemented by position of primer (P), positive control (+) (all natural dNTPs are present), and two negative controls (absence of either natural dATP (**A−**) or dUTP (**U−**)). The full length products (**ON17**) contain four modified **dA^{R}** or **dU^{R}** nucleotides.

Table 3. Melting Temperatures of DNA Duplexes

duplex	T_m (°C)	ΔT_m,[a] (°C)
ON1/ON13	73.6	0
ON1/ON13 dA^{BIF}	70.6	−3.0
ON1/ON13 dA^{BFU}	70.7	−2.9
ON1/ON13 dA^{BOX}	70.5	−3.1
ON1/ON13 dA^{ABOX}	70.1	−3.5
ON2/ON15	73.3	0
ON2/ON15 dU^{BFU}	70.4	−2.9
ON2/ON15 dU^{BOX}	71.1	−2.2
ON2/ON15 dU^{ABOX}	71.2	−2.1
ON3/ON4	75.6	0
ON3/ON4 dU^{BFU}	72.6	−3.0
ON3/ON4 dU^{BOX}	72.7	−2.9
ON3/ON4 dU^{ABOX}	72.7	−2.9
ON6/ON7	84.6	0
ON6/ON7 dU^{BFU}	81.3	−3.3
ON6/ON7 dU^{BOX}	81.4	−3.2
ON6/ON7 dU^{ABOX}	81.4	−3.2
ON17/ON18	81.2	0
ON17/ON18 dA^{BFU}	68.3	−3.2
ON17/ON18 dA^{BOX}	69.4	−2.9
ON17/ON18 dU^{BOX}	72.1	−2.3

[a]$\Delta T_m = (T_{mmod} - T_{mnat})/n_{mod}$. The biaryl functionalized nucleosides exert moderate destabilizing effect around 2−3 °C per modified base.

that these three model compounds possess the important photophysical features of the full nucleoside systems and enable us to explain significantly different (and solvent-dependent) Stokes shifts in the measured emission spectra. In the gas-phase, presumably the most accurate spectra (absorption and emission) were obtained using RI-CC2 method that should represent the most rigorous (and still, computationally tractable) method

dx.doi.org/10.1021/jo202321g | J. Org. Chem. 2012, 77, 1026−1044

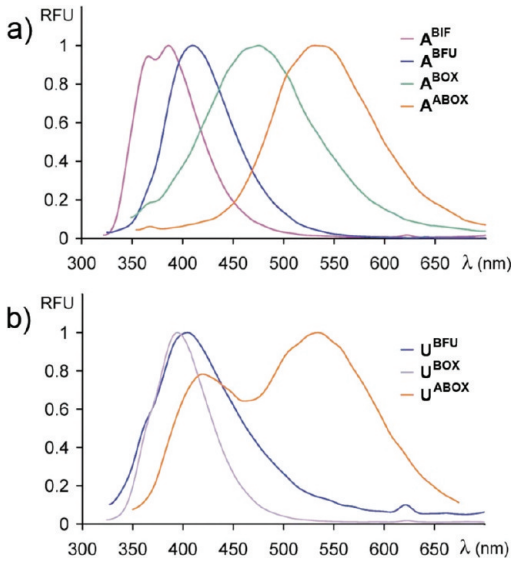

Figure 2. Normalized emission spectra of the 10 μM modified nucleosides in methanol. (a) The emission spectra of $\mathbf{dA^R}$ nucleosides. $\mathbf{dA^{BIF}}$ (λ_{em} = 366, 386 nm), $\mathbf{dA^{BFU}}$ (λ_{em} = 409 nm), $\mathbf{dA^{BOX}}$ (λ_{em} = 475 nm), and $\mathbf{dA^{ABOX}}$ (λ_{em} = 535 nm). (b) The emission spectra of $\mathbf{dU^R}$ nucleosides. $\mathbf{dU^{BFU}}$ (λ_{em} = 402 nm), $\mathbf{dU^{BOX}}$ (λ_{em} = 392 nm), and $\mathbf{dU^{ABOX}}$ (λ_{em} = 422, 538 nm). The emission spectra were measured by excitation at 320 nm (310 nm for $\mathbf{dA^{BIF}}$, 340 nm for $\mathbf{dA^{BOX}}$ and $\mathbf{dN^{ABOX}}$).

Table 4. Photophysical Properties of the Modified Nucleosides in Methanol

$\mathbf{dN^R}$	λ_{abs}	ε (L mol^{-1} cm^{-1})	λ_{em}	Φ_F
$\mathbf{dA^{BIF}}$	286	23000	366, 386	0.73
$\mathbf{dA^{BFU}}$	323	36000	409	0.66
$\mathbf{dA^{BOX}}$	321	26000	475	0.10
$\mathbf{dA^{ABOX}}$	280, 327	22400, 16000	535	0.12
$\mathbf{dU^{BIF}}$	288	18000		
$\mathbf{dU^{BFU}}$	318	38000	402	0.11
$\mathbf{dU^{BOX}}$	312	33000	392	0.52
$\mathbf{dU^{ABOX}}$	301	25000	422, 538	0.10

available for the systems containing 40−50 atoms. The solvent effects (solvatochromic shifts) were then evaluated using TD-DFT method (CAM-B3LYP functional that is assumed to yield satisfactorily accurate description of the excited states with significant charge transfer character) and SMD solvation model according to the multistep protocol described in the Computational Details. The results of the calculations are summarized in Table 5.

Several observations can be made from the data presented in Table 5. Absorption spectra are predicted to a good accuracy by both methods, more accurate RI-CC2 and cheaper TD-DFT-(CAM-B3LYP). In agreement with the experimental data, solvatochromic shifts in the absorption spectra are quite small, with the largest being computed for $\mathbf{MeA^{ABOX}}$ (λ_{abs} = 311 nm in the gas-phase vs 330 nm in acetonitrile, CAM-B3LYP values).

Large Stokes shifts in the emission spectra can be explained by a combination of two factors: solvatochromic shifts and the change in nuclear coordinates between S_0 and S_1 equilibrium geometries. The latter is largest for the $\mathbf{MeA^{ABOX}}$ with λ_{em}(RI-CC2, gas-phase) = 414 nm (cf., λ_{abs} = 326 nm), whereas it is smaller for the other two systems. When analyzed in more details, the S_1 stabilization (i.e., the difference in the energy of

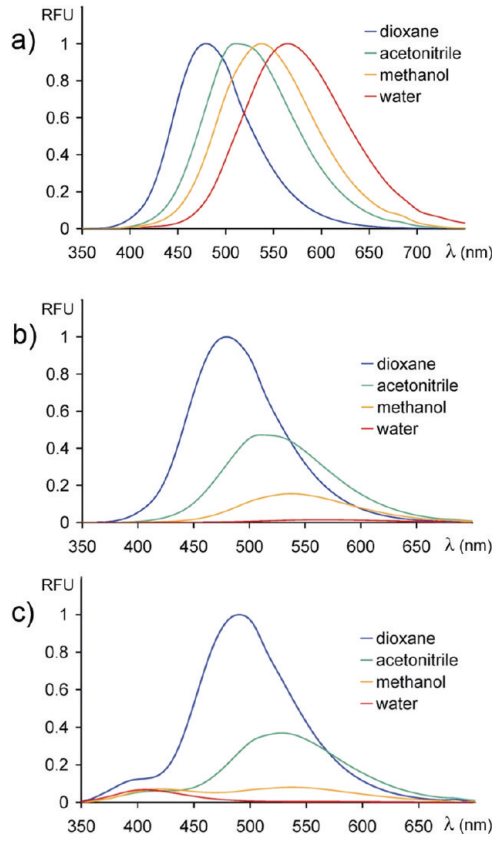

Figure 3. Solvatochromic properties of 5 μM $\mathbf{dN^{ABOX}}$ in various solvents. (a) Normalized emission spectra of $\mathbf{dA^{ABOX}}$ in different solvents: dioxane (λ_{em} = 480 nm), acetonitrile (λ_{em} = 515 nm), methanol (λ_{em} = 535 nm), and water (λ_{em} = 565 nm). (b) Relative emission spectra of $\mathbf{dA^{ABOX}}$ in different solvents: dioxane (Φ = 0.62), acetonitrile (Φ = 0.35), methanol (Φ = 0.12), and water (Φ = 0.009). (c) Relative emission spectra of $\mathbf{dU^{ABOX}}$ in different solvents: dioxane (λ_{em} = 491 nm, Φ = 0.69), acetonitrile (λ_{em} = 528 nm, Φ = 0.32), methanol (λ_{em} = 422, 538 nm, Φ = 0.10), and water (λ_{em} = 406 nm, Φ = 0.008). The emission spectra were measured by excitation at 340 nm.

Table 5. Calculated Photophysical Properties of Three Model Compounds, $\mathbf{MeA^{ABOX}}$, $\mathbf{MeA^{BOX}}$, and $\mathbf{MeA^{BFU}}$, and Comparison with Experimental Data

environment	method		$\mathbf{MeA^{ABO-X}}$	$\mathbf{MeA^{BOX}}$	$\mathbf{MeA^{BFU}}$
gas-phase	RI-CC2	λ_{abs} (*osc strength*)	326 nm (*0.77*)	314 (*0.88*)	308 (*1.11*)
	CAM-B3LYP	λ_{abs}	311 (*0.90*)	305 (*0.88*)	305 (*1.13*)
	RI-CC2	λ_{em}	414	372	361
	CAM-B3LYP	λ_{em}	369	364	364
1,4-dioxane	CAM-B3LYP	λ_{abs} (λ_{abs}-*exp*)	320 (*349*)[a]	311 (*325*)[b]	313 (*327*)[c]
	CAM-B3LYP	λ_{em} (λ_{em}-*exp*)	391 (*480*)[a]	361 (*432*)[b]	348 (*403*)[c]
acetonitrile	CAM-B3LYP	λ_{abs} (λ_{abs}-*exp*)	330 (*339*)[a]	317 (*322*)[b]	321 (*322*)[c]
	CAM-B3LYP	λ_{em} (λ_{em}-*exp*)	477 (*515*)[a]	404 (*469*)[b]	376 (*423*)[c]

[a]Experimental emission maxima for $\mathbf{dA^{ABOX}}$. [b]Experimental emission maxima for $\mathbf{dA^{BOX}}$. [c]Experimental emission maxima for $\mathbf{dA^{BFU}}$.

the first excited state in the ground state geometry and in its optimized geometry) in the $\mathbf{MeA^{ABOX}}$ accounts for 3363 cm^{-1}

dx.doi.org/10.1021/jo202321g | J. Org. Chem. 2012, 77, 1026−1044

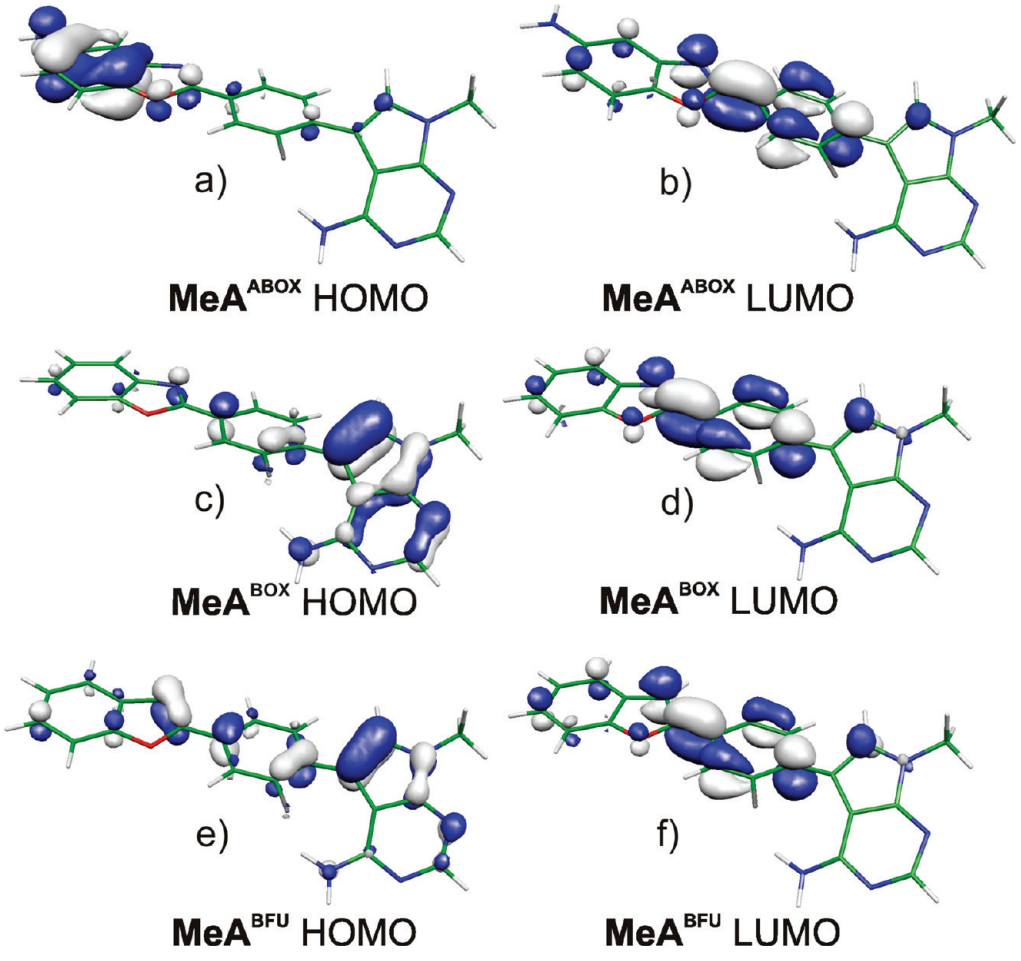

Figure 4. Frontier molecular orbitals for (a, b) **MeA**^{ABOX} , (c, d) **MeA**^{ABOX}, and (d, e) **MeA**^{BFU} systems.

whereas the S_0 destabilization for approximately the same value, 3137 cm^{-1} (yielding a total of 6500 cm^{-1} as the calculated *in vacuo* Stokes shift). Corresponding values for **MeA**^{BOX} and **MeA**^{BFU} are 4962 and 4757 cm^{-1}. The geometrical change responsible for the greater Stokes shift in **MeA**^{ABOX} is planarization of the NH_2 group on benzoxazole ring upon excitation. Unfortunately, these trends are not quantitatively reproduced by more approximate TD-DFT(CAM-B3LYP) calculations. What is, however, nicely reproduced, are the observed solvatochromic shifts, as can be seen from the calculated values of λ_{em} values presented in Table 5. In relative scale (i.e., as the differences between the calculated *in vacuo* and solvent values compared to their experimental counterparts in nonpolar and polar solvents), these shifts are reproduced almost quantitatively. We explain the observed trends by the different character of the excitation between **MeA**^{ABOX} and **MeA**^{BOX} on one hand and **MeA**^{BFU} on the other hand as depicted in Figure 4. The dominant excitations in the RI-CC2 ansatz are always from HOMO to LUMO orbital (contributing 85−91% in the RI-CC2 wave function). As can be seen in Figure 4, the character of LUMO is almost the same in all three fluorophores and is mostly localized on the fluorobenzene moiety and the bond connecting the two aryl rings. The HOMO is, however, localized mostly on aminobenzoxazole (**MeA**^{ABOX} due to the presence of the electron-donating amino goup) or adenine (**MeA**^{BOX}) rings, whereas it is more delocalized in the case of **MeA**^{BFU}. It suggests that a greater charge-transfer character of the S_1−S_0 excitation can be expected for **MeA**^{ABOX} and **MeA**^{BOX}, whereas it is more of a rather valence-type excitation in the case of **MeA**^{BFU}. Quantitatively, it is exemplified by the difference in the dipole moments of the ground and excited states, which were calculated to be $\Delta\mu$ = 9.45, 8.79, and 4.88 D for **MeA**^{ABOX}, **MeA**^{BOX}, and **MeA**^{BFU}, respectively. In other words, introduction of the N-heteroatom to the benzofurane moiety (from **MeA**^{BFU} to **MeA**^{BOX}) and even further the addition of electron-donating amino group (in **MeA**^{ABOX}) largely increase the dipole moment of the excited state and thus increase the Stokes shifts. It is well-known that the solvatochromic shifts are much smaller for the absorption spectra (despite the fact that the individual μ's for three studied systems are of the comparable magnitude to their emission counterparts) since the absorption is the fast process and solvent does not have time to reorient itself to effectively solvate the more polar excited states.

Photophysical Properties of the Modified dNTPs and the Effect of pH. Absorption and emission spectra of the modified **dN**^{R}**TPs** were measured in water (Table 6) at different pH values. At pH = 7, they showed lower intensity of fluorescence compared to modified nucleosides in methanol. Some functional groups of the fluorophores can be protonated or deprotonated depending on pH, which influences the electronic densities of the fluorophores. Modified **dA**^{R}**TPs** contain one amino group (pK_a = 5.2[18]) at the deazaadenosine moiety, whereas **dN**^{ABOX}**TP** derivatives possess one extra amino group at the biaryl moiety. Consistently with the pK_a, the fluorescence changes within a range of slightly acidic pH values (4−6).

dx.doi.org/10.1021/jo202321g | J. Org. Chem. 2012, 77, 1026−1044

Table 6. Photophysical Properties of Modified dN^{R}TPs in Water with Respect to pH

			pH = 3		pH = 7		pH = 10	
dN^{R}TP	λ_{abs}	ε (L mol^{-1} cm^{-1})	λ_{em}	Φ_F	λ_{em}	Φ_F	λ_{em}	Φ_F
dA^{BIF}TP	287	21000			409	0.23	409	0.23
dA^{BFU}TP	320	35000			437	0.28	437	0.28
dA^{BOX}TP	319	27000	429	0.13	496	0.015	496	0.015
dA^{ABOX}TP[a]	280, 336	21000, 22000	443	0.01	565	0.01	565	0.01
dU^{BIF}TP	287	17000						
dU^{BFU}TP	315	37000					366, 386	0.21
dU^{BOX}TP	310	31000	391	0.18	391	0.18	427	0.54
dU^{ABOX}TP[b]	293	21000	406	0.81	406, 560	0.002	560	0.02

[a] dA^{ABOX}TP has λ_{abs} = 318 nm (ε = 27000 L mol^{-1} cm^{-1}) at pH = 3. [b] dU^{ABOX}TP has λ_{abs} = 308 nm (ε = 25000 L mol^{-1} cm^{-1}) at pH = 3.

Replacement of an electron-donating amino group with an electron-withdrawing ammonium group in acidic environment causes the decrease of electronic densities and results in the fluorescence quenching of **dA^{BIF}TP** (Figure S14 in Supporting Information) and **dA^{BFU}TP** (Figure 5a). In contrast, **dA^{BOX}TP** becomes more emissive with one extra violet emission (λ_{em} = 429 nm) in the slightly acidic environment, which covers less intense green emission (λ_{em} = 496 nm) in neutral or basic environment (Figure 5b). A similar effect of increase of fluorescence can be observed for **dA^{ABOX}TP** upon protonation of the additional amino group causing an interesting dual fluorescent behavior (Figure 5c). In neutral and basic environment, the fluorophore has yellow emission caused by the electron donating amino group (λ_{em} = 565 nm). When the pH is lowered, the yellow emission decreases until it disappears (due to the protonation of the amino group), while an increase of another blue emission at 443 nm (resembling the emission of protonated **dA^{BOX}TP**) can be observed. The observed green emission at pH = 4.5 originates from presence of both forms. The fluorescence increase of **dA^{ABOX}** absorption spectra differed only in **dN^{ABOX}TP** due to a stronger effect of electron charge transfer upon protonation of amino group at the **ABOX** moiety (Figure S17 in Supporting Information).

Modified **dU^{R}TPs** were characterized by lower fluorescence intensities compared to the modified **dA^{R}TPs**. At neutral conditions, **dU^{BFU}TP** is nonfluorescent, whereas **dU^{ABOX}TP** exerts a low fluorescence (Table 3, Figure 6a,c). Uridine moiety contains an imido group, which is slightly acidic (pK_a = 9.25),[19] and therefore the proton is abstracted in slightly basic environment to cause an increase of intensity of fluorescence, which is not accompanied by a significant change of UV spectra. Both **dU^{BFU}TP** and **dU^{BOX}TP** showed a high increase of fluorescence in basic environment, while the **dU^{BOX}TP** even changed its emission maximum (Figure 6a,b). In contrast, **dU^{ABOX}TP** exhibited different pH dependence (Figure 6c). When the environment is changed from neutral to basic (pH = 10), the yellow emission (λ_{em} = 560 nm) is highly increased (in accord with the other **dU^{R}TP** derivatives). However, in acidic solutions, a new highly intense violet emission (λ_{em} = 406 nm) appears due to the protonation of the amino group. This also explains the major band of **dU^{ABOX}** emission at the neutral pH that is due to the presence of a low amount of highly intense **dU^{ABOX}** protonated form. Further changes to more acidic conditions cause strong enhancement of the **dU^{ABOX}** violet emission (accompanied by change of UV spectrum, Figure S17).

Photophysical Properties of the Biaryl-Labeled DNA. Single-stranded oligonucleotides (ssONs, **ON1** or **ON2**) containing either one of the four **dA^{R}** or one of the four **dU^{R}** modifications (all combinations were made) were prepared by primer extension on biotinylated template followed by

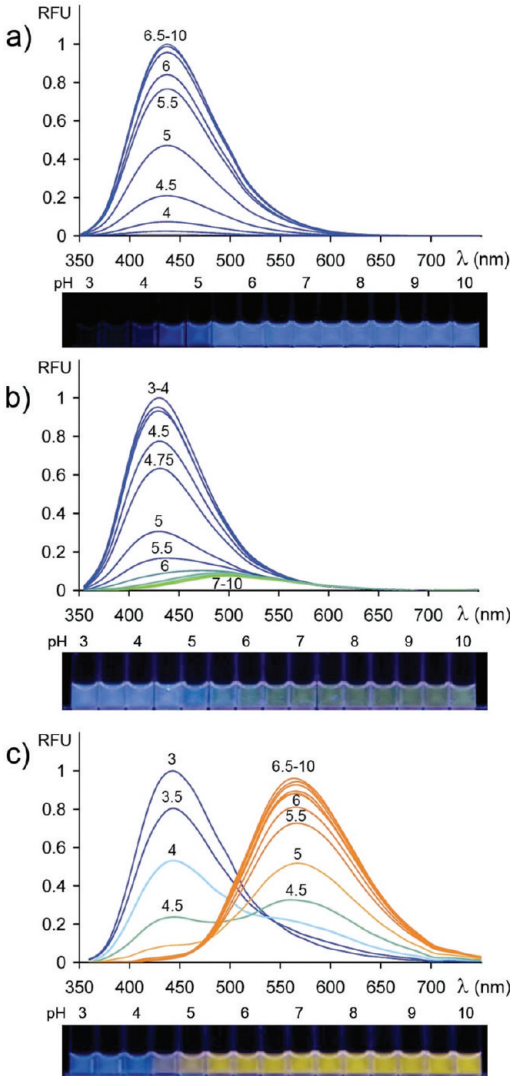

Figure 5. Photophysical properties of (a) 12 μM **dA^{BFU}TP**, (b) 22 μM **dA^{BOX}TP**, (c) 30 μM **dA^{ABOX}TP** in the range of pH = 3−10. Emission spectra were measured by excitation at 340 nm. In contrast to methanolic solutions, the fluorophores exert red-shifted emission maxima in aqueous neutral and basic conditions **dA^{BFU}TP** (λ_{em} = 437), **dA^{BOX}TP** (λ_{em} = 496) nm, **dA^{ABOX}TP** (λ_{em} = 565 nm). In acidic environment, fluorescence of **dA^{BFU}TP** diminishes upon protonation of 7-deazaadenosine moiety, while **dA^{BOX}TP** and **dA^{ABOX}TP** enhance blue emissions (λ_{em} = 429, 443 nm, respectively).

dx.doi.org/10.1021/jo202321g | J. Org. Chem. 2012, 77, 1026−1044

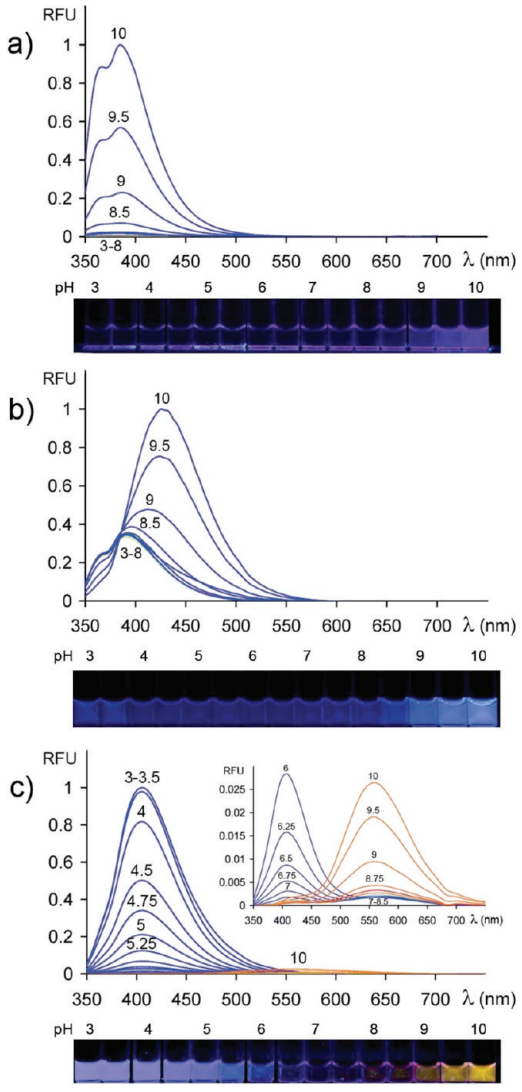

Figure 6. Fluorescence spectra of (a) 20 μM **dU^{BFU}TP**, (b) 25 μM **dU^{BOX}TP**, (c) 30 μM **dU^{ABOX}TP** in the range of pH = 3–10. The emission spectra were measured by excitation at 330 nm. In neutral environment, **dU^{BFU}TP** is nonemissive, **dU^{BOX}TP** exerts violet emission (λ_{em} = 391 nm), and **dU^{ABOX}TP** has very low dual emission (λ_{em} = 406, 560 nm). The emission intensity of all modified **dUTPs** is significantly enhanced upon deprotonation of the uridine moiety in basic environment. After deprotonation **dU^{BFU}TP** exerts violet emission (λ_{em} = 366, 386 nm). Additionaly, **dU^{ABOX}TP** exerts a significant enhancement of violet emission (λ_{em} = 406 nm) in acidic environment upon the protonation of the amino group of **ABOX** moiety.

magnetoseparation[15] of the modified ssON. The sequence was selected for its high electron-donating properties containing guanosine flanking nucleobases, which have lowest oxidation potential of all bases.[20] Easy oxidation of adjacent guanosines often leads to significant decrease of fluorescence intensity of intrinsically fluorescent nucleoside analogues causing problems with detection and applications.[21] This phenomenon was also utilized for the identification of mismatches by guanine-specific fluorescence quenching caused by intercalation of pyrene fluorophore to DNA strand upon mismatch formation.[22] The biaryl-substituted nucleosides were therefore studied for mismatch and deletion studies with respect to the effect of guanosine electron-rich flanking sequence.

Emissions of fluorescent **dA^{R}** nucleotides incorporated to ssONs (PEX products) exhibit blue-shifted emission maxima, which resemble emission spectra in methanol and indicate increased hydrophobicity. This behavior may be explained by the stacking of the fluorophore-containing nucleobase in single-strand DNA and minor exposure of the fluorophore to aqueous environment (Figures 2a and 7a). The stacking interactions

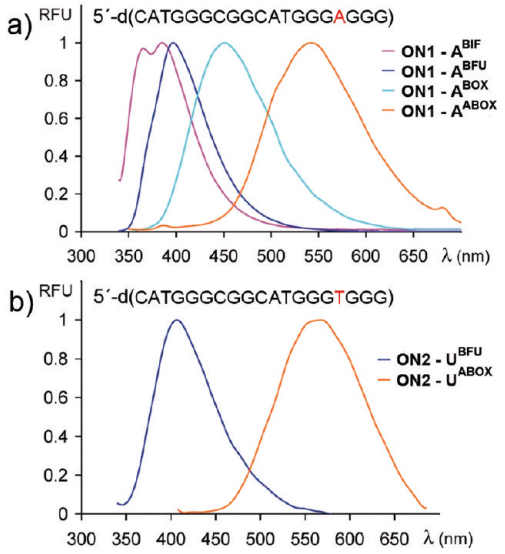

Figure 7. Photophysical properties of (a) **ON1** functionalized by **dA^{BIF}** and **dA^{BFU}** exerted blue-shifted emissions with lower fluorescence intensity compared to free fluorophores (λ_{em} = 364, 386, and 397 nm; Φ = 0.09 and 0.18). Emission maxima of **ON1** functionalized by **dA^{BOX}** and **dA^{ABOX}** are blue-shifted but with significantly higher emission intensity compared to free fluorophores (λ_{em} = 451, 535 nm; Φ = 0.1, 0.08). (b) **ON2** sequence functionalized by quenched **dU^{BOX}** and violet- and yellow-emitting **dU^{BFU}** and **dU^{ABOX}** (λ_{em} = 406, 554 nm; Φ = 0.02, 0.01). The emission spectra were measured by excitation at 330 nm (340 nm for **dN^{ABOX}**, **dA^{BOX}**) in 20 mM phosphate buffer, pH = 6.

induce also different response of **dA^{R}TP** fluorescence intensity after incorporation of fluorophores into the DNA strand. The incorporation of **dA^{BOX}** and **dA^{ABOX}** to ONs led to an increase of fluorescence intensity, which corresponds to the presence of adjacent stacked nucleotides and lower access to aqueous environment. In the contrast, **dA^{BIF}** and **dA^{BFU}** show a decrease of emission upon incorporation to ONs. This could be attributed to the electronic effect of the flanking guanosine nucleotides (Figure 7a).

Modified **dU^{R}** showed different fluorescence properties after incorporation to DNA compared to the corresponding **dU^{R}TPs**. In neutral aqueous conditions, **dU^{BFU}TP** was nonfluorescent, **dU^{BOX}TP** exerted violet emission (λ_{em} = 391 nm), and **dU^{ABOX}TP** gave violet emission of its ionized form (λ_{em} = 406 nm) (Figure 6a–c). However, in the **ON2** sequence, the DNA containing **dU^{BFU}** was fluorescent (λ_{em} = 401 nm), while **dU^{BOX}**-labeled DNA was almost nonfluorescent and the **dU^{ABOX}**-DNA exerted only the enhanced yellow fluorescence (λ_{em} = 554 nm) of its nonionized form at pH = 6 (Figures 6c and 7b). The quenching of **dU^{BOX}** and **dU^{ABOX}** acidic forms in **ON2** sequence can be attributed to the effect of fluorescence quenching by the flanking guanosine nucleotides.

Effect of Structural Changes in DNA on the Fluorescence of the Labels. Since the fluorescent properties of

dx.doi.org/10.1021/jo202321g | J. Org. Chem. 2012, 77, 1026–1044

the free fluorophores in water differ from the properties of stacked fluorophores within DNA (particularly in the case of **dU**^{R} derivatives), further studies of the influence of the structural changes of DNA on the fluorescence have been conducted. The model example was the conversion of a hairpin to double-strand DNA (dsDNA) after addition of the complementary strand. We have chosen the hairpin structure of which the loop structure had been previously determined by NMR spectroscopy (Figure 8).[23] The stem was designed as

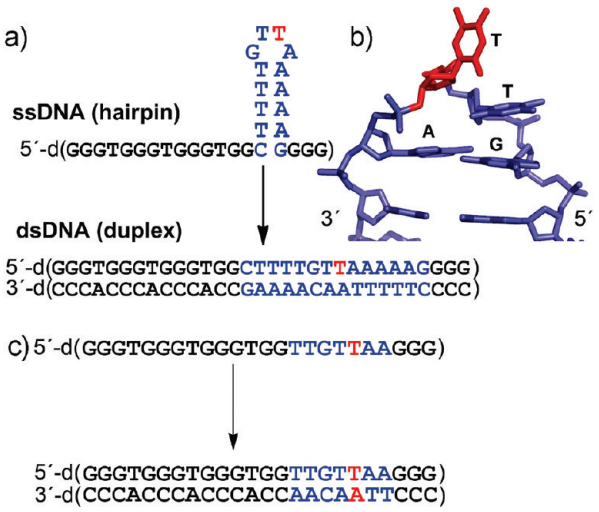

Figure 8. (a) Sequences used for hairpin (the modified nucleotide in red)−dsDNA transition. (b) Detail of the NMR structure of the loop region.[23] (c) A reference sequence (with the same flanking nucleotides) not forming hairpin structure.

weakly bound and consisted of four A-T and one C-G base pairs in order to get efficient dissociation of the hairpin stem and duplex formation. The sequence of bases in the loop was selected according to the published NMR structure, where the second T in the unpaired GTTA region is exposed to the solution. Therefore the DNA containing a modified **dU**^{R} at this position was expected to exert significant changes of fluorescence upon hybridization. Single-strand oligonucleotides (**ON3**) containing **dU**^{BFU}, **dU**^{BOX}, and **dU**^{ABOX} in the loop position were prepared by the PEX on biotinylated template followed by magnetoseparation[15] of the modified ssON. The fluorescence spectra (Figure 9) were recorded at pH = 6 in the absence and in the presence of the complementary strand (**ON4**).

Interestingly, the **dU**^{BFU} fluorophore in the hairpin structure still showed relatively high intensity of fluorescence (Φ = 0.035) in comparison with nonfluorescent **dU**^{BFU}, indicating the presence of some interactions even in the loop region (Figure 9a, red curve). The lack of guanosine nucleotides in the flanking sequence of the **ON3** oligonucleotide leads to an enhancement of the **dU**^{R} violet fluorescence. Hence, the violet emissions of **dU**^{BOX} as well as the minor acidic form of **dU**^{ABOX} are not diminished. The **dU**^{BOX} fluorophore exerts violet emission (λ_{em} = 366 and 387 nm), and **dU**^{ABOX} emits dual emission (λ_{em} = 401, 560 nm) (Figure 9b,c, red curves). In all cases, the intensity of fluorescence of the incorporated **dU**^{R} increased by the factor of 1.6−3.4 after addition of the complementary strand, which indicates the base-pair formation and higher hindrence to uridine moiety of fluorophores toward water molecules upon duplex formation (Figure 9a−c, blue curves). Due to the absence of flanking guanosines, the acidic form of

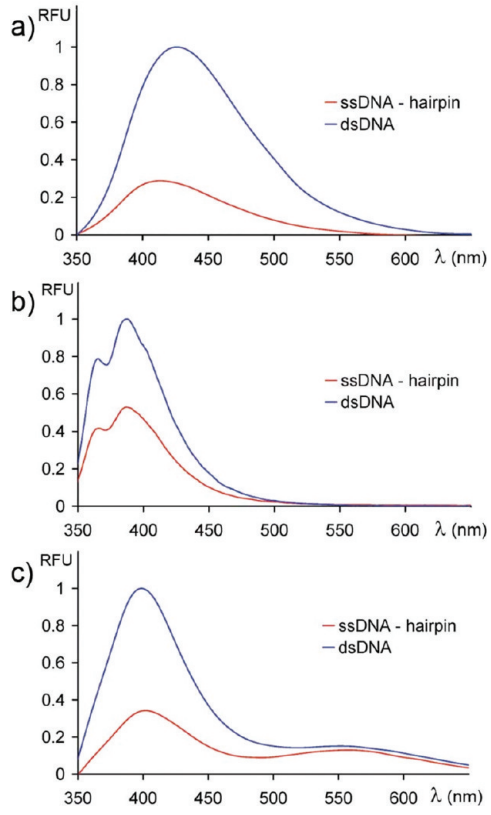

Figure 9. Fluorescence spectra of 7 μM **ON3** (pH = 6) containing hairpin (ssDNA) and hybridized with **ON4** to form double-stranded DNA (dsDNA). Labeled **ON3** showed enhanced intensity of fluorescence upon hybridization with **ON4** given by ratios between intensities of ssDNA and duplex. **ON3** was labeled by (a) **dU**^{BFU}: $\Phi_{dsDNA}/\Phi_{ssDNA}$ = 0.12/0.035 = 3.4, hairpin (λ_{em} = 413 nm), dsDNA (λ_{em} = 427 nm); (b) **dU**^{BOX}: $\Phi_{dsDNA}/\Phi_{ssDNA}$ = 0.095/0.06 = 1.6, λ_{em} = 366, 386 nm; (c) **dU**^{ABOX}: $\Phi_{dsDNA}/\Phi_{ssDNA}$ = 0.02/0.008 = 2.5, λ_{em} = 406 nm. The emission spectra were measured by excitation at 340 nm (330 nm for **dU**^{BOX}) in 20 mM phosphate buffer, pH = 6.

dU^{ABOX} gives the major increase in fluorescence upon hybridization (Figure 9c).

The **dU**^{R} fluorophores were also studied in hybridization of **ON5** oligonucleotide containing the same flanking sequence without a possibility of forming a hairpin structure (Figure S19 in Supporting Information). **dU**^{BOX} and **dU**^{ABOX} show only a minor increase of fluorescence intensity upon hybridization ($\Phi_{dsDNA}/\Phi_{ssDNA}$ = 1.05, 1.2) compared to **ON3** oligonucleotide ($\Phi_{dsDNA}/\Phi_{ssDNA}$ = 1.6, 2.5), respectively. On the other hand, **dU**^{BFU} showed a stronger increase of fluorescence upon duplex formation ($\Phi_{dsDNA}/\Phi_{ssDNA}$ = 1.85), indicating that **dU**^{BFU} reflects the base-pair formation more sensitively than other fluorophores.

Mismatch Studies. **ON1** and **ON2** oligonucleotide sequences were selected for the complete study of all modified nucleotides for use in the detection of single nucleotide mismatches. The ONs containing one modified **dA**^{R} or one modified **dU**^{R} were synthesized by PEX with magnetoseparation as in the previous cases. They were hybridized with a matching sequence and all three mismatch sequences (the mismatch was the opposite to the modified nucleotide). All modified **dA**^{R} showed similar behavior of the fluorescence response to the particular type of mismatch (Figure 10 and Table S1 in Supporting Information). When the **dA**^{R} was opposite to matching T, the

dx.doi.org/10.1021/jo202321g | J. Org. Chem. 2012, 77, 1026−1044

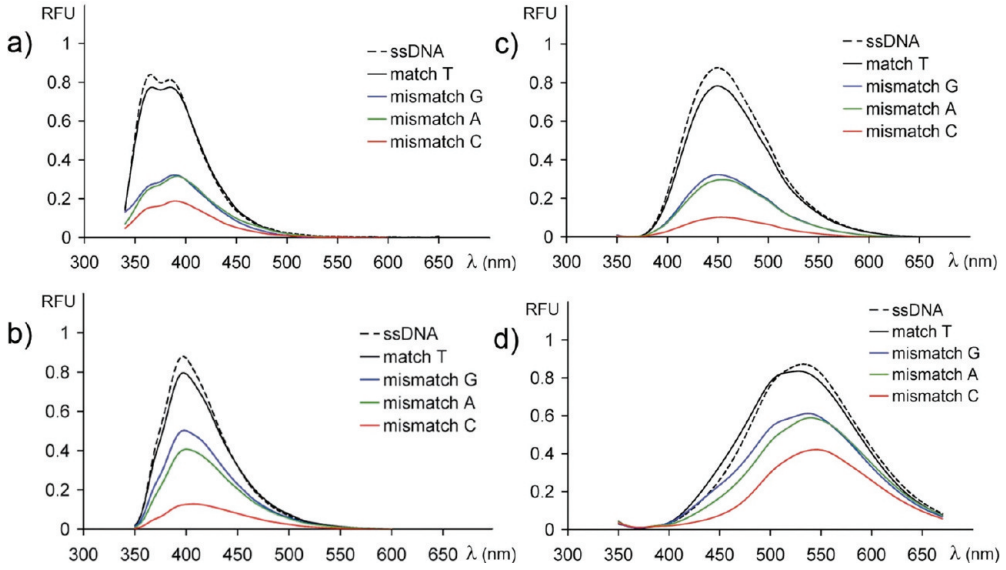

Figure 10. Fluorescence spectra of 7 μM **ON1** functionalized by (a) **dA**^{BIF}, (b) **dA**^{BFU}, (c) **dA**^{BOX}, and (d) **dA**^{ABOX} hybridized with complementary strand containing T (**ON13**), G (**ON14**), A (**ON15**), and C (**ON16**) in the opposite position of the complementary strand. Intensity of fluorescnce was decreased by about 7−14% in perfectly matched duplex. Mismatched duplexes containing G and A led to a 33−64% and 37−68% decrease of fluorescence intensity, respectively. The C mismatch led to a 79−87% drop of fluorescence intesity. Detailed data available is provided in the Supporting Information. The emission spectra were measured by excitation at 340 nm (320 nm for **dA**^{BIF}) in 20 mM phosphate buffer, pH = 6.

intensity of fluorescence was about the same or slightly (7−14%) lower compared to ssDNA. On the other hand, when any mismatch base was opposite to the modification, a significant drop in fluorescence intensity was observed. The mismatch of G or A opposite to **dA**^{R} led to a 33−68% decrease in fluorescence, whereas the C mismatch exerted in even a more pronounced effect (79−87% drop in intensity). The **dA**^{BIF} and **dA**^{BOX} gave generally the strongest base discrimination compared to **dA**^{BFU} and **dA**^{ABOX}.

The behavior of **dU**^{R} modifications was slightly different. **dU**^{BIF} and **dU**^{BOX} were not fluorescent in this particular DNA sequence. **dU**^{BFU} and **dU**^{ABOX} were suitable for the base-discrimination study (Figure 11a, Figure S18 and Table S1 in Supporting Information). Perfectly matched dsDNA containing **dU**^{BFU} or **dU**^{ABOX} fluorophores showed ca. 23−41% decrease of fluorescence compared to ssDNA. Interestingly, the T-**dU**^{R} mismatch showed only a small drop of intensity (2−18%) compared to ssDNA and stronger fluorescence compared to matched dsDNA. The other two mismatches (C and G) gave a significant (77−79%) drop in the fluorescence intensity. To determine whether this T-**dU**^{R} mismatch dichotomy is sequence-dependent, we studied the effect of the slightly less electron-donating flanking CG nucleotides in the PvuII sequence to the sensitivity of **dU**^{BFU} fluorescence with respect to a mismatch formation. (Figure 10, **ON6** vs **ON10**−**ON12**). In this particular sequence, the match dsDNA slightly increased intensity of fluorescence of **dU**^{BFU} compared to ssDNA, whereas all mismatches decreased the emission intensities by 25−35% (Figure 11b). Apparently, even the **dU**^{BFU} modification is able to sense the mismatches, and the effect is sequence-dependent. The lower discrimination may be attributed to different flanking CG nucleotides with lower electron donating properties compared to the GG flanking nucleotides.

Effect of pH on the Photophysical Properties of dsDNA. The dual fluorescence of the **dA**^{ABOX} and **dU**^{ABOX} modifications was also studied in dsDNA at pH = 4−7 and 10 (Figure 12 and Figure S20 in Supporting Information). At neutral and basic

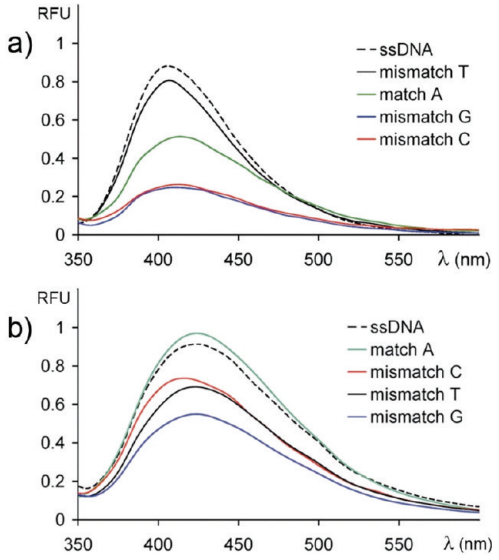

Figure 11. Fluorescence spectra of (a) 7 μM **ON2** functionalized by **dU**^{BFU} hybridized with complementary strand containing T (**ON13**), G (**ON14**), A (**ON15**), and C (**ON16**) in the opposite position of the complementary strand. The perfectly matched duplex decreased intensity of fluorescence about 41%. Mismatched duplexes containing T, G, and C led to 18%, 77%, and 79% decrease of fluorescence intensity, respectively. (b) Fluorescence spectra of 7 μM **ON6** containing **dU**^{BFU} hybridized perfectly matched sequence (**ON7**) and sequences containing C mismatch (**ON10**), T mismatch (**ON11**), and G mismatch (**ON12**). Perfectly matched duplex led to a 15% increase of fluorescence compared to single-stranded oligonucleotide, and duplexes containing C, T, and G mismatches led to a 16%, 24%, and 35% decrease of fluorescence intensity, respectively. The emission spectra were measured by excitation at 330 nm in 20 mM phosphate buffer, pH = 6.

conditions, both modifications exert a yellow emission (λ_{em} = 545, 555 nm). Under basic conditions, no significant increase in fluorescent intensity was observed (compared to high increase

dx.doi.org/10.1021/jo202321g | J. Org. Chem. 2012, 77, 1026−1044

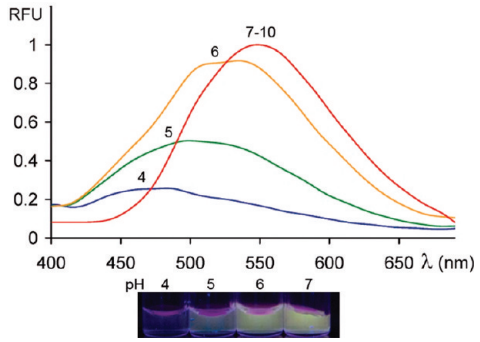

Figure 12. Fluorescence spectra of 2 μM **dA^{ABOX}**-labeled **ON1**/**ON13** duplex at different pH = 4−10. Under neutral or basic conditions (pH = 7−10) **dA^{ABOX}** modified oligonucleotide displays yellow emission (λ_{em} = 550 nm). The emission maxima of **dA^{ABOX}** are decreased upon protonation of the amino group with significant blue shift in acidic environment at pH = 6 (λ_{em} = 535 nm), pH = 5 (λ_{em} = 499 nm), and pH = 4 (λ_{em} = 483 nm). The emission spectra were measured by excitation at 340 nm in 20 mM phosphate buffer at pH = 4, 5, 6, 7, and 10.

in **dU^{ABOX}TP** by deprotonation, vide supra). Apparently, the intensity of the fluorescence is not significantly affected by deprotonation in duplex DNA because of the $\pi-\pi$ stacking effect of flanking nucleobases. On the other hand, under acidic conditions (pH = 4), the **dA^{ABOX}** and **dU^{ABOX}** emissions are decreased by protonation of the amino group of the label, and a weak blue fluorescence at 483 or 490 nm can be observed. While the **dU^{ABOX}** retains its standard yellow emission upon protonation of its amino group (Figure S20 in Supporting Information), the emission of **dA^{ABOX}** is blue-shifted on the protonation (Figure 12). The emission maxima are significantly blue-shifted, when acidity is increased. The fluorescence is changed from yellow at pH = 7 (λ_{em} = 550 nm) and pH = 6 (λ_{em} = 535 nm), to green at pH = 5 (λ_{em} = 499 nm) and finally to blue at pH = 4 (λ_{em} = 483 nm). This unusual pH sensitivity (continually blue-shifted emission with decreasing pH values) can be attributed to a dual blue and yellow emissions of different excited states of protonated and deprotonated forms of **dA^{ABOX}** in combination with the $\pi-\pi$ stacking effect of the DNA duplex and the quenching effect of the flanking G nucleotides. Further acidifying to pH = 3 and below did not change the emission maxima and may lead to depurination of DNA.

^{19}F NMR Spectroscopy. The ^{19}F NMR spectra of modified dNTPs and ss- and dsDNA were studied. The chemical shift of **dU^{ABOX}** (−122.1 ppm) incorporated into ssDNA exerts a significant difference from the free **dU^{ABOX}TP** with the chemical shift of −108.9 ppm in water (Figure 13). This change in chemical shift can be attributed to $\pi-\pi$ stacking within DNA and can also be in accordance with presence of some $\pi-\pi$ stacking within single-stranded DNA. The same chemical shift of **dU^{ABOX}** (ca. −122 ppm) was also observed in dsDNA (not shown).

Detection of Structural Changes by ^{19}F NMR Spectroscopy. Since the chemical shift of **dU^{ABOX}TP** (−108.9 ppm) in water differs by ca. 13 ppm from $\pi-\pi$ stacked **dU^{ABOX}** (−122.1 ppm) in ss- or dsDNA, it can be assumed that ^{19}F NMR spectroscopy could be a good method for detection of the modification in the hairpin structure (where little $\pi-\pi$ stacking is expected). Therefore, the **ON3** containing **dU^{ABOX}** was measured by itself and after hybridization with a complementary strand (**ON4**, Figures 14 and S21 in Supporting

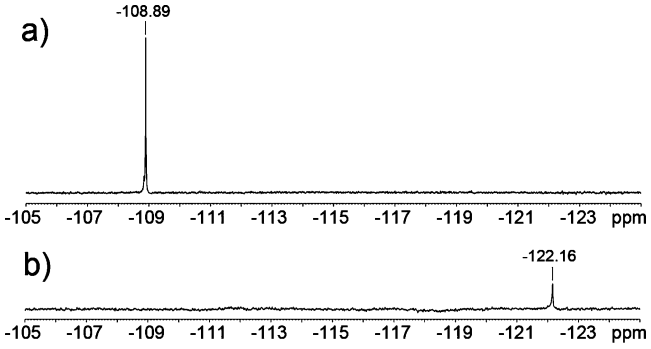

Figure 13. ^{19}F NMR spectra of (a) 5 mM **dU^{ABOX}TP** as a representative of unstacked ^{19}F NMR labels with chemical shift at −108.9 ppm; (b) 40 μM **dU^{ABOX}**-labeled **ON2** and **ON2**/**ON15** duplex exerting identical significantly upfield-shifted ^{19}F NMR signal at −122.1 ppm compared to unincorporated free **dU^{ABOX}TP**. Spectra were measured in 20 mM phosphate buffer at pH = 7.

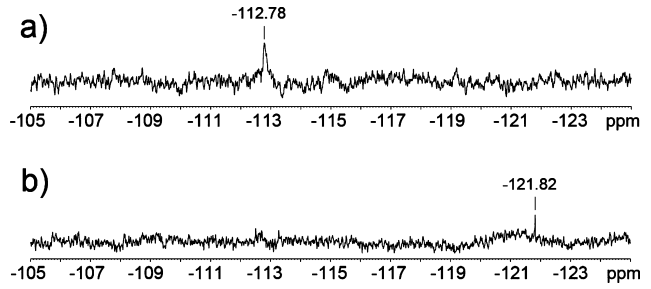

Figure 14. ^{19}F NMR spectra of (a) 30 μM **ON3** containing **dU^{ABOX}**-labeled hairpin structure with downfield shifted ^{19}F NMR signal at −112.7 ppm originated from distortion of $\pi-\pi$ stacking; (b) 30 μM **ON3** after addition of **ON4** resulting in dissolution of a hairpin structure and **ON3**/**ON4** duplex formation accompanied by upfield shifted ^{19}F NMR signal to −121.8 ppm. Spectra were measured in 20 mM phosphate buffer at pH = 7.

Information). Indeed, the hairpin ssDNA containing **dU^{ABOX}** gave a ^{19}F NMR signal at −112.8 ppm, whereas after addition of **ON4**, the signal was shifted to −121.8 ppm. Apparently, the ^{19}F NMR spectroscopy of the **dU^{ABOX}** in DNA can distinguish between the hairpin and stacked ss- or dsDNA. However, it should be noted that at the rather low concentrations of ONs prepared by enzymatic incorporations in PEX, the intensity of the ^{19}F NMR signals are quite low and relatively long acquisition times (12−48 h) are needed to get good spectra.

■ CONCLUSIONS

Eight novel nucleosides **dA^{R}**, **dU^{R}** and nucleoside triphosphates **dA^{R}TP**, **dU^{R}TP** bearing multimode fluorescent and ^{19}F NMR detectable **BIF**, **BFU**, **BOX**, and **ABOX** labeling groups were designed and prepared by single-step aqueous cross-coupling reactions of halogenated nucleosides or dNTPs with biarylboronates. All of the modified **dN^{R}TP**s were good substrates for KOD XL polymerase, and the PEX incorporations were used for synthesis of modified DNA. The modified **dN^{R}** exerted interesting fluorescent properties, and some of them were very sensitive to the environment and/or to the secondary structures of DNA. The emission maxima of different modified adenosine (**dA^{R}**) nucleosides range from 370 to 540 nm in methanol. **dA^{BIF}** exhibited fluorescence emission at λ_{em} = 366 and 386 nm. The more conjugate and electron-rich benzofurane derivative (**dA^{BFU}**) shifts fluorescence emission to

dx.doi.org/10.1021/jo202321g | J. Org. Chem. 2012, 77, 1026−1044

λ_{em} = 409 nm, introduction of a N-heteroatom (**dA^{BOX}**) led to significant red shift to λ_{em} = 475 nm, and further addition of an electron-donating amino group (**dA^{ABOX}**) caused further red-shifted yellow fluorescent emission (λ_{em} = 535 nm). The Stokes shifts were found up to 200 nm. Calculations have revealed that the major effect caused by the introduction of another N-heteroatom and additional amino group is based on increased differences of the dipole moments of the frontier orbitals, which manifest in larger charge-transfer character of the excitation and thus in larger Stokes shifts. The modified uridine (**dU^{R}**) nucleosides are generally blue-shifted (compared to **dA^{R}**), but **dU^{BIF}** is nonfluorescent, whereas **dU^{ABOX}** exerts dual fluorescence. Both **dN^{ABOX}** have solvatochromic fluorescent properties, showing bathochromic shift about 85 nm with increasing polarity from dioxane to water and 70-fold decrease in emission intensity. Fluorescence of modified **dN^{R}TPs** depends also on pH owing to the presence of acidic or basic groups. The most interesting were **dA^{BOX}TP**, **dA^{ABOX}TP**, and **dU^{ABOX}TP** possessing dual character of fluorescence changing from yellow or green in neutral or slightly basic environment to blue or violet in acidic environment. This dual fluorescence could be used for the study of pH microenvironments in the range from 4 to 6 for **dA^{R}TP** and 5.5 to 9 for **dU^{R}TP**. The fluorophores incorporated to DNA are able to sense the changes in the structure of the DNA strand by the increase of intensity in fluorescence during the transformation from hairpin to double strand, which has been confirmed simultaneously by ^{19}F NMR measurement. The fluorophores are also able to detect the site-specific single nucleotide mismatches in the G-rich sequence by decrease of intensity of fluorescence. However, the effects are sequence-dependent. The best fluorophore for study of structural changes is **dU^{BFU}**, which is only slightly fluorescent when exposed to water (hairpin or deletions) but gives good emission in ss- or dsDNA. The fluorescence of **dU^{R}** nucleosides depends on the flanking sequence. The most electron-donating flanking guanosine nucleotides cause decreasing **dU^{BFU}** fluorescence and quenching of the **dU^{BOX}** and **dU^{ABOX}** violet emissions. Several modifications **dA^{BIF}**, **dA^{BOX}**, and **dU^{BFU}** showed base-discrimination in the sequence containing adjacent guanosine and thus could be used for mismatch detection in electron-donating flanking sequences. **dA^{ABOX}** and **dU^{ABOX}** are solvatochromic and can be used as sensors of the polarity of DNA microenvironment, i.e., in binding studies with other biomolecules. The **dA^{ABOX}** fluorophore in DNA is extraordinarily sensitive to acidic pH. It shows a continual blue shift of the emission maxima upon the protonation in acidic environment. Particularly interesting and important is a change of emission maxima in the range of pH = 7, 6, 5 (λ_{em} = 550, 535, and 499 nm), which makes it possible to visually distinguish between pH 6 and 5. Therefore, the **dA^{ABOX}** could be a useful tool for fine pH sensing in biological systems. Studies along these lines will continue in our laboratory.

EXPERIMENTAL SECTION

NMR spectra were recorded on a 600 MHz (600 MHz for ^{1}H, 564 MHz for ^{19}F, 240.2 MHz for ^{31}P, 151 MHz for ^{13}C) or a 500 MHz (500 MHz for ^{1}H, 470.4 MHz for ^{19}F, 200.2 MHz for ^{31}P, 125.8 MHz for ^{13}C) spectrometer from sample solutions in D_2O, DMSO-d_6, methanol-d_4, or acetone-d_6. Chemical shifts (in ppm, δ scale) were referenced to the solvent signal (D_2O, referenced to dioxane 3.75 ppm, pH = 7.1 for ^{1}H NMR and to H_3PO_4 0.00 ppm for ^{31}P NMR; acetone-d_6, 2.05 ppm for ^{1}H NMR and 29.8 ppm (CD_3 group of acetone-d_6) for ^{13}C NMR; $CDCl_3$, 7.26 ppm for ^{1}H NMR and 77.36 ppm for ^{13}C NMR; methanol-d_4, 3.34 ppm for ^{1}H NMR and 49.86 ppm for ^{13}C NMR; DMSO-d_6, 2.54 ppm for ^{1}H NMR and 40.45 ppm (CD_3 group of DMSO-d_6) for ^{13}C NMR). Coupling constants (J) are given in Hz. NMR spectra of dNTPs were measured in phosphate buffer at pH 7.1. Complete assignment of all NMR signals was achieved by using a combination of H,H−COSY, H,C-HSQC, and H,C-HMBC experiments. Mass spectra were measured by ESI. Semipreparative separation of nucleoside triphosphates was performed by HPLC on a column packed with 10 μm C18 reversed phase (Phenomenex, Luna C18 (2)). IR spectra were measured using KBr tabletes. High resolution mass spectra were measured using ESI ionization technique. Mass spectra of functionalized DNA were measured by MALDI-TOF, with nitrogen laser. UV−vis spectra were measured at room temperature.

4-Bromo-3-fluoro-4′-methoxybiphenyl (1a). DMF (4 mL) was added to argon-purged flask containing 4-methoxyphenylboronic acid (302 mg, 2 mmol, 1 equiv) 1-bromo-2-fluoro-4-iodobenzene (720 mg, 2.4 mmol, 1.2 equiv), $Pd(PPh_3)_2Cl_2$ (68 mg, 0.1 mmol, 0.05 mol %) and K_2CO_3 (414 mg, 4 mmol, 2 equiv). The mixture was stirred at 80 °C for 5 h then evaporated and product was purified by silica gel column chromatography using hexane-ethylacetate (0−10%) as eluent. The product was isolated as white solid (429 mg, 74%). ^{1}H NMR (600 MHz, $CDCl_3$): 3.86 (s, 3H, CH_3O); 6.98 (m, 2H, H-3′,5′); 7.21 (ddd, 1H, $J_{5,6}$ = 8.3, $J_{5,3}$ = 2.1, $J_{H,F}$ = 0.7, H-5); 7.30 (dd, 1H, $J_{H,F}$ = 10.0, $J_{3,5}$ = 2.1, H-3); 7.49 (m, 2H, H-2′,6′); 7.56 (dd, 1H, $J_{6,5}$ = 8.3, $J_{H,F}$ = 7.3, H-6). ^{13}C NMR (151 MHz, $CDCl_3$): 55.4 (CH_3O); 107.0 (d, $J_{C,F}$ = 21, C-1); 114.4 (CH-3′,5′); 114.5 (d, $J_{C,F}$ = 23, CH-3); 123.3 (d, $J_{C,F}$ = 3, CH-5); 128.0 (CH-2′,6′); 131.4 (d, $J_{C,F}$ = 2, C-1′); 133.6 (CH-6); 142.3 (d, $J_{C,F}$ = 7, C-4); 159.3 (d, $J_{C,F}$ = 247, C-2); 159.8 (C-4′). ^{19}F NMR (470.3 MHz, $CDCl_3$): −108.0. MS (ESI$^+$): m/z (%) 280 (100) $[M + H]^+$, 282 (97) $[M + H]^+$. HR-MS (ESI$^+$) for $C_{13}H_{10}OBrF$: $[M + H]^+$ calculated 279.9899, found 279.9907. IR: 2841, 1608, 1581, 1559, 1522, 1478, 1394, 1309, 1292, 1268, 1249, 1201, 1187, 1119, 1030, 891, 871, 838, 808, 694.

2-(4′-Bromo-3′-fluorophenyl)-1-benzofuran (1b). DMF (4 mL) was added to argon-purged flask containing benzofuran boronic acid (322 mg, 2 mmol, 1 equiv), 1-bromo-2-fluoro-4-iodobenzene (720 mg, 2.4 mmol, 1.2 equiv), $Pd(PPh_3)_2Cl_2$ (68 mg, 0.1 mmol, 5 mol %), and K_2CO_3 (414 mg, 4 mmol, 2 equiv). The mixture was stirred at 80 °C for 5 h and then evaporated, and product was purified by silica gel column chromatography using hexane as eluent. The product was isolated as white solid (491 mg, 85%). ^{1}H NMR (499.8 MHz, $CDCl_3$): 6.98 (d, 1H, $J_{3,7}$ = 1.0, H-3); 7.18 (ddd, 1H, $J_{5,4}$ = 7.7, $J_{5,6}$ = 7.3, $J_{5,7}$ = 1.0, H-5); 7.25 (ddd, 1H, $J_{6,7}$ = 8.1, $J_{6,5}$ = 7.3, $J_{6,4}$ = 1.4, H-6); 7.44 (m, 2H, H-7 and H-6′); 7.52 (ddd, 1H, $J_{4,5}$ = 7.7, $J_{4,6}$ = 1.4, $J_{4,7}$ = 0.8, H-4); 7.54 (dd, 1H, $J_{H,F}$ = 9.6, $J_{2',6'}$ = 2.0, H-2′); 7.54 (dd, 1H, $J_{5',6'}$ = 8.3, $J_{H,F}$ = 6.9, H-5′).^{13}C NMR (125.7 MHz, $CDCl_3$): 102.8 (CH-3); 108.9 (d, $J_{C,F}$ = 21.1, C-4′); 111.3 (CH-7); 112.7 (d, $J_{C,F}$ = 24.5, CH-2′); 121.2 (CH-4); 121.5 (d, $J_{C,F}$ = 3.5, CH-6′); 123.3 (CH-5); 125.0 (CH-6); 128.8 (C-3a); 131.7 (d, $J_{C,F}$ = 7.7, C-1′); 133.9 (CH-5′); 153.6 (d, $J_{C,F}$ = 2.5, C-2); 154.9 (C-7a); 159.4 (d, $J_{C,F}$ = 247.1, C-3′). ^{19}F NMR (470.3 MHz, $CDCl_3$): −107.1 (dd, $J_{F,H}$ = 9.6, 6.9). MS (ESI$^+$): m/z (%) 290 (100) $[M + H]^+$, 292 (97) $[M + H]^+$. HR-MS (ESI$^+$) for $C_{14}H_8OBrF$: $[M^+]$ calculated 289.9743, found 289.9751. IR: 1609, 1556, 1483, 1472, 1453, 1426, 1397, 1350, 1289, 1260, 1218, 1190, 1168, 1054, 945, 869, 812, 750, 684.

2-(4′-Bromo-3′-fluorophenyl)-1,3-benzoxazole (1c). Polyphosphoric acid (20 g) was added to flask containing 2-aminophenol (218 mg, 2 mmol, 1 equiv) and 4-bromo-3-fluorobenzoic acid (438 mg, 2 mmol, 1 equiv). The reaction mixture was heated at 170 °C for 16 h. After cooling the reaction mixture was diluted by water and neutralized by concentrated solution of KOH, and formed precipitate was filtered and washed by water and dried. The product was isolated as white solid (516 mg, 89%). ^{1}H NMR (499.8 MHz, $CDCl_3$): 7.38 (m, 1H, H-5); 7.40 (m, 1H, H-6); 7.59 (m, 1H, H-7); 7.72 (dd, 1H, $J_{5',6'}$ = 8.3, $J_{H,F}$ = 6.8, H-5′); 7.78 (m, 1H, H-4); 7.93 (dd, 1H, $J_{6',5'}$ = 8.3, $J_{6',2'}$ = 1.9, H-6′); 8.00 (dd, 1H, $J_{H,F}$ = 9.0, $J_{2',6'}$ = 1.9, H-2′). ^{13}C NMR (125.7 MHz, $CDCl_3$): 110.7 (CH-7); 112.9 (d, $J_{C,F}$ = 21.2, C-4′); 115.4 (d, $J_{C,F}$ = 25.0, CH-2′); 120.3 (CH-4); 124.1 (d, $J_{C,F}$ = 3.7, CH-6′); 125.0 (CH-5); 125.8 (CH-6); 128.3 (d, $J_{C,F}$ = 7.7, C-1′); 134.3 (CH-5′); 141.8 (C-3a); 150.8 (C-7a); 159.3 (d, $J_{C,F}$ = 248.3, C-3′); 161.0 (d, $J_{C,F}$ = 3.4, C-2). ^{19}F NMR (470.3 MHz, $CDCl_3$): −101.7 (dd, $J_{F,H}$ = 9.0, 6.8). MS (ESI$^+$): m/z (%) 292 (100) $[M + H]^+$, 294 (97)

dx.doi.org/10.1021/jo202321g | J. Org. Chem. 2012, 77, 1026−1044

$[M + H]^+$. HR-MS (ESI^+) for $C_{13}H_8ONBrF$: $[M + H]^+$ calculated 291.9768, found 291.9768. IR: 3077, 1620, 1599, 1555, 1484, 1471, 1454, 1427, 1401, 1347, 1307, 1243, 1191, 1180, 1066, 1038, 1003, 943, 885, 825, 786.

5-Amino-2-(4′-bromo-3′-fluorophenyl)-1,3-benzoxazole (1d). Polyphosphoric acid (20 g) was added to flask containing 2,4-diaminophenol hydrochloride (394 mg, 2 mmol, 1 equiv) and 4-bromo-3-fluorobenzoic acid (438 mg, 2 mmol, 1 equiv). The reaction mixture was heated at 170 °C for 16 h. After cooling the reaction mixture was diluted by water and neutralized by concentrated solution of KOH, and formed precipitate was filtered and washed by water and dried. The product was isolated as yellow solid (567 mg 94%). ^1H NMR (499.8 MHz, $CDCl_3$): 3.76 (bs, 2H, NH_2); 6.74 (dd, 1H, $J_{5,4}$ = 8.6, $J_{5,7}$ = 2.3, H-5); 7.03 (dd, 1H, $J_{7,5}$ = 2.3, $J_{7,4}$ = 0.4, H-7); 7.35 (dd, 1H, $J_{4,5}$ = 8.6, $J_{4,7}$ = 0.4, H-4); 7.69 (dd, 1H, $J_{5',6'}$ = 8.3, $J_{H,F}$ = 6.8, H-5′); 7.87 (ddd, 1H, $J_{6',5'}$ = 8.3, $J_{6',2'}$ = 2.0, $J_{H,F}$ = 0.8, H-6′); 7.95 (dd, 1H, $J_{H,F}$ = 9.2, $J_{2',6'}$ = 2.0, H-2′). ^{13}C NMR (125.7 MHz, $CDCl_3$): 105.0 (CH-7); 110.8 (CH-4); 112.5 (d, $J_{C,F}$ = 21.0, C-4′); 114.4 (CH-5); 115.2 (d, $J_{C,F}$ = 25.0, CH-2′); 124.0 (d, $J_{C,F}$ = 3.6, CH-6′); 128.5 (d, $J_{C,F}$ = 7.7, C-1′); 134.2 (CH-5′); 142.9 (C-7a); 144.2 (C-6); 144.8 (C-3a); 159.3 (d, $J_{C,F}$ = 248.1, C-3′); 161.4 (d, $J_{C,F}$ = 2.7, C-2). ^{19}F NMR (470.3 MHz, $CDCl_3$): −102.0 (dd, $J_{F,H}$ = 9.2, 6.8). MS (ESI^+): *m/z* (%) 307 (99) $[M + H]^+$, 309 (100) $[M + H]^+$. HR-MS (ESI^+) for $C_{13}H_9N_2OBrF$: $[M^+]$ calculated 306.9877, found 306.9878. IR: 3404, 3334, 1630, 1604, 1553, 1482, 1451, 1427, 1398, 1351, 1305, 1272, 1214, 1185 1167, 1067, 1037, 962, 887, 860, 804, 723, 617.

General Procedure for Borylation Reaction. Dioxane (5 mL) was added to an argon-purged flask containing aryl halide **1a−1d** (1 mmol, 1 equiv), $PdCl_2$(dppf) (36.5 mg, 0.05 mmol, 5 mol %), bis-(pinacolato)diboron B_2Pin_2 (506 mg, 2 mmol, 2 equiv), and potassium acetate (294 mg, 3 mmol, 3 equiv). The reaction mixture was stirred at 80 °C for 4 h and then evaporated, and the product was purified by silica gel column chromatography using hexane/ethylacetate (0−20%) as eluent. The isolated product contained also unreacted B_2Pin_2. Since the pinacolatoesters are prone to hydrolysis by slightly acidic silica gel and B_2Pin_2 does not interfere with subsequent Suzuki coupling, the products were not repurified. The yields were calculated according ratio of signals of B_2Pin_2 and products from NMR spectra.

4-Pinacolatoboronyl-3-fluoro-4′-methoxybiphenyl (2a). **2a** was prepared according to the general procedure, **1a** (281 mg, 1 mmol, 1 equiv) and B_2Pin_2 (506 mg, 2 mmol, 2 equiv). The product was isolated as white solid (269 mg, 203 mg of **2a**, 62%). ^1H NMR (499.8 MHz, DMSO-d_6): 1.30 (s, 12H, $(CH_3)_2C$); 3.80 (s, 3H, CH_3O); 7.03 (m, 2H, H-*m*-C_6H_4OMe); 7.42 (dd, 1H, $J_{H,F}$ = 11.1, $J_{3,5}$ = 1.6, H-3); 7.49 (dd, 1H, $J_{5,6}$ = 7.7, $J_{5,3}$ = 1.6, H-5); 7.68 (dd, 1H, $J_{6,5}$ = 7.7, $J_{H,F}$ = 6.4, H-6); 7.69 (m, 2H, H-*m*-C_6H_4OMe). ^{13}C NMR (125.7 MHz, DMSO-d_6): 24.8 ($(CH_3)_2C$); 55.5 (CH_3O); 83.9 ($(CH_3)_2C$); 112.7 (d, $J_{C,F}$ = 24.6, CH-3); 113.4 (C-1); 114.7 (CH-*m*-C_6H_4OMe); 121.8 (d, $J_{C,F}$ = 2.6, CH-5); 128.3 (CH-*o*-C_6H_4OMe); 130.7 (d, $J_{C,F}$ = 2.1, C-*i*-C_6H_4OMe); 137.3 (d, $J_{C,F}$ = 8.8, CH-6); 145.7 (d, $J_{C,F}$ = 8.7, C-4); 159.9 (C-*p*-C_6H_4OMe); 167.3 (d, $J_{C,F}$ = 249.3, C-2). $^{19}F\{^1H\}$ NMR (470.3 MHz, DMSO-d_6): −102.5. MS (ESI^+): *m/z* (%) 361.1 (10) $[M + Na]^+$. HR-MS (ESI^+) for $C_{20}H_{20}O_3BFNa$: $[M + Na]^+$ calculated 361.1382, found 361.1370.

2-(4′-Pinacolatoboronyl-3′-fluorophenyl)-1-benzofuran (2b). **2b** was prepared according to the general procedure, **1b** (291 mg, 1 mmol, 1 equiv) and B_2Pin_2 (1 g, 4 mmol, 4 equiv). An additional 2 equiv of B_2Pin_2 were used to increase the conversion of the reaction. The product was isolated as white solid (720 mg, 199 mg of **2b**, 59%). ^1H NMR (499.8 MHz, acetone-d_6): 1.36 (s, 12H, CH_3); 7.28 (ddd, 1H, $J_{5,4}$ = 7.8, $J_{5,6}$ = 7.2, $J_{5,7}$ = 1.0, H-5); 7.37 (ddd, 1H, $J_{6,7}$ = 8.3, $J_{6,5}$ = 7.2, $J_{6,4}$ = 1.3, H-6); 7.48 (d, 1H, $J_{3,7}$ = 1.0, H-3); 7.60 (dtd, 1H, $J_{7,6}$ = 8.3, $J_{7,5}$ = $J_{7,3}$ = 1.0, $J_{7,4}$ = 0.7, H-7); 7.62 (dd, 1H, $J_{H,F}$ = 10.3, $J_{2',6'}$ = 1.4, H-2′); 7.68 (ddd, 1H, $J_{4,5}$ = 7.8, $J_{4,6}$ = 1.3, $J_{4,7}$ = 0.7, H-4); 7.77 (dd, 1H, $J_{6',5'}$ = 7.7, $J_{6',2'}$ = 1.4, H-6′); 7.82 (dd, 1H, $J_{5',6'}$ = 7.7, $J_{H,F}$ = 6.0, H-5′). ^{13}C NMR (125.7 MHz, acetone-d_6): 25.1 ($(CH_3)_2C$); 84.67 ($C(CH_3)_2$); 104.7 (CH-3); 111.9 (d, $J_{C,F}$ = 26.8, CH-2′); 112.0 (CH-7); 116.9 (C-4′); 120.7 (d, $J_{C,F}$ = 2.9, CH-6′); 122.3 (CH-4); 124.2 (CH-5); 126.1 (CH-6); 129.8 (C-3a); 136.2 (d, $J_{C,F}$ = 9.2, C-1′); 138.4 (d, $J_{C,F}$ = 8.7, CH-5′); 154.9 (d, $J_{C,F}$ = 2.7, C-2); 155.8 (C-7a); 168.3 (d, $J_{C,F}$ = 250.4, C-3′). ^{19}F NMR (470.3 MHz, acetone-d_6): −103.1 (dd, $J_{F,H}$ = 10.3, 6.0). MS (ESI^-): *m/z* (%) 351.2 (45) $[M + Na]^+$. HR-MS (ESI^+) for $C_{19}H_{22}O_3BFNa$: $[M + Na]^+$ calculated 351.1538, found 351.1531.

2-(4′-Pinacolatoboronyl-3′-fluorophenyl)-1,3-benzoxazole (2c). **2c** was prepared according to the general procedure, **1c** (292 mg, 1 mmol, 1 equiv) and B_2Pin_2 (506 mg, 2 mmol, 2 equiv). The product was isolated as white solid (340 mg, 229 mg of **2c**, 65%). ^1H NMR (500.0 MHz, CD_3OD): 1.39 (s, 12H, $(CH_3)_2C$); 7.42 (td, 1H, $J_{5,4}$ = $J_{5,6}$ = 7.3, $J_{5,7}$ = 1.4, H-5-benzoxazole); 7.46 (td, 1H, $J_{6,5}$ = $J_{6,7}$ = 7.3, $J_{6,4}$ = 1.4, H-6-benzoxazole); 7.70 (ddd, 1H, $J_{7,6}$ = 7.3, $J_{7,5}$ = 1.4, $J_{7,4}$ = 0.7, H-7-benzoxazole); 7.76 (ddd, 1H, $J_{4,5}$ = 7.3, $J_{4,6}$ = 1.4, $J_{4,7}$ = 0.7, H-4-benzoxazole); 7.88 (dd, 1H, $J_{H,F}$ = 9.7, $J_{3,5}$ = 1.4, H-3-C_6H_3F); 7.89 (t, 1H, $J_{6,5}$ = $J_{H,F}$ = 7.7, H-6-C_6H_3F); 8.03 (dd, 1H, $J_{5,6}$ = 7.7, $J_{5,3}$ = 1.4, H-5-C_6H_3F). ^{13}C NMR (125.7 MHz, CD_3OD): 25.2 ($(CH_3)_2C$); 85.6 ($C(CH_3)_2$); 112.0 (CH-7-benzoxazole); 115.0 (d, $J_{C,F}$ = 27.2, CH-3-C_6H_3F); 121.0 (CH-4-benzoxazole); 123.7 (d, $J_{C,F}$ = 3.3, CH-5-C_6H_3F); 126.3 (CH-5-benzoxazole); 127.3 (CH-6-benzoxazole); 132.8 (d, $J_{C,F}$ = 9.1, C-4-C_6H_3F); 138.8 (CH-6-C_6H_3F); 142.8 (C-3a-benzoxazole); 152.1 (C-7a-benzoxazole); 163.0 (C-2-benzoxazole); 168.5 (d, $J_{C,F}$ = 251.5, C-2-C_6H_3F); (C-1-C_6H_3F not detected). ^{19}F NMR (470.3 MHz, CD_3OD): −108.9 (dd, $J_{F,H}$ = 9.7, 7.7). MS (ESI^+): *m/z* (%) 340.2 (13) $[M + H]^+$. HR-MS (ESI^+) for $C_{19}H_{20}O_3NBF$: $[M + H]^+$ calculated 340.1515, found 340.1509.

5-Amino-2-(4′-pinacolatoboronyl-3′-fluorophenyl)-1,3-benzoxazole (2d). **2d** was prepared according to the general procedure, **1d** (307 mg, 1 mmol, 1 equiv) and B_2Pin_2 (506 mg, 2 mmol, 2 equiv). The product was isolated as yellow solid (494 mg, 261 mg of **2d**, 74%). ^1H NMR (499.8 MHz, CD_3OD): 1.38 (s, 12H, $(CH_3)_2C$); 6.86 (dd, 1H, $J_{5,4}$ = 8.7, $J_{5,7}$ = 2.3, H-5); 7.05 (dd, 1H, $J_{7,5}$ = 2.3, $J_{7,4}$ = 0.7, H-7); 7.41 (dd, 1H, $J_{4,5}$ = 8.7, $J_{4,7}$ = 0.7, H-4); 7.80 (dd, 1H, $J_{H,F}$ = 9.7, $J_{2',6'}$ = 1.4, H-2′); 7.86 (dd, 1H, $J_{5',6'}$ = 7.8, $J_{H,F}$ = 5.9, H-5′); 7.96 (ddd, 1H, $J_{6',5'}$ = 7.8, $J_{6',2'}$ = 1.4, H-6′). ^{13}C NMR (125.7 MHz, CD_3OD): 25.2 ($(CH_3)_2C$); 85.6 ($(CH_3)_2C$); 105.5 (CH-7); 111.8 (CH-4); 114.6 (d, $J_{C,F}$ = 27.1, CH-2′); 116.4 (CH-5); 120.4 (C-4′); 123.4 (d, $J_{C,F}$ = 3.1, CH-6′); 133.1 (d, $J_{C,F}$ = 9.1, C-1′); 138.7 (d, $J_{C,F}$ = 8.3, CH-5′); 143.54 (C-7a); 145.7 (C-6); 147.1 (C-3a); 163.1 (d, $J_{C,F}$ = 3.3, C-2); 168.5 (d, $J_{C,F}$ = 251.4, C-3′). ^{19}F NMR (470.3 MHz, $CDCl_3$): −99.2 (dd, $J_{F,H}$ = 9.7, 5.9). MS (ESI^+): *m/z* (%) 355.2 (100) $[M + H]^+$. HR-MS (ESI^+) for $C_{19}H_{21}O_3N_2BF$: $[M + H]^+$ calculated 355.1624, found 355.1620.

General Procedure for Suzuki Cross-Coupling of Base-Halogenated Nucleoside Analogues (dN^I) with Biaryl Pinacolatoboronates. A mixture of H_2O/CH_3CN (2:1, 2 mL) was added to an argon-purged flask containing nucleoside analogue $\mathbf{dN^I}$ (75 μmol), a boronate (110 μmol, 1.5 equiv adjusted to the amount of boronate), and Cs_2CO_3 (73 mg, 225 μmol, 3 equiv). In a separate flask, $Pd(OAc)_2$ (0.84 mg, 3.75 μmol, 5 mol %) and P(Ph-SO_3Na)$_3$ (5.39 mg, 9.37 μmol, 2.5 equiv to Pd) were combined, and the flask was evacuated and purged with argon followed by addition of H_2O/CH_3CN (2:1, 0.5 mL). The mixture of catalyst was then injected to the reaction mixture, and the reaction mixture was stirred at 80 °C for 2 h. The products were isolated by silica gel column chromatography using chloroform/methanol (0−10%) as eluent.

7-Deaza-7-[(3″-fluoro-4‴-methoxy-[1″,1‴-biphenyl]-4″-yl)]-2′-deoxyadenosine (dA^{BIF}). $\mathbf{dA^{BIF}}$ was prepared according to the general procedure, $\mathbf{dA^I}$ (28.2 mg, 0.075 mmol), **2a** (47 mg, 0.11 mmol). The product was isolated as white solid (20 mg, 61%). ^1H NMR (500.0 MHz, CD_3OD): 2.37 (ddd, 1H, J_{gem} = 13.4, $J_{2'b,1'}$ = 6.0, $J_{2'b,3'}$ = 2.6, H-2′b); 2.73 (ddd, 1H, J_{gem} = 13.4, $J_{2'a,1'}$ = 8.2, $J_{2'a,3'}$ = 6.0, H-2′a); 3.74 (dd, 1H, J_{gem} = 12.1, $J_{5'b,4'}$ = 3.7, H-5′b); 3.82 (dd, 1H, J_{gem} = 12.1, $J_{5'a,4'}$ = 3.3, H-5′b); 3.84 (s, 3H, CH_3O); 4.04 (ddd, 1H, $J_{4',5'}$ = 3.7, 3.3, $J_{4',3'}$ = 2.6, H-4′); 4.55 (dt, 1H, $J_{3',2'}$ = 6.0, 2.6, $J_{3',4'}$ = 2.6, H-3′); 6.59 (dd, 1H, $J_{1',2'}$ = 8.2, 6.0, H-1′); 7.02 (m, 2H, H-*m*-C_6H_4OMe); 7.47 (t, 1H, $J_{6,5}$ = $J_{H,F}$ = 8.0, H-6-C_6H_3F); 7.49 (dd, 1H, $J_{H,F}$ = 11.5, $J_{3,5}$ = 1.5, H-3-C_6H_3F); 7.50 (d, 1H, $J_{H,F}$ = 0.7, H-6-deazapurine); 7.52 (dd, 1H, $J_{5,6}$ = 8.0, $J_{5,3}$ = 1.9, H-5-C_6H_3F); 7.63 (m, 2H, H-*o*-C_6H_4OMe); 8.14 (s, 1H, H-2-deazapurine). ^{13}C NMR (125.7 MHz, CD_3OD): 41.5 (CH_2-2′); 55.8 (CH_3O); 63.7 (CH_2-5′); 73.1 (CH-3′); 86.7 (CH-1′); 89.2 (CH-4′); 103.7 (C-4a-deazapurine); 114.8 (d, $J_{C,F}$ = 23.2, CH-3-C_6H_3F); 115.5 (CH-*m*-C_6H_4OMe); 120.9 (d, $J_{C,F}$ = 15.8, C-1-C_6H_3F);

dx.doi.org/10.1021/jo202321g | J. Org. Chem. 2012, 77, 1026−1044

123.6 (d, $J_{C,F}$ = 3.2, CH-5-C_6H_3F); 124.1 (d, $J_{C,F}$ = 2.1, CH-6-deazapurine); 129.0 (CH-*o*-C_6H_4OMe); 132.8 (d, $J_{C,F}$ = 1.9, C-*i*-C_6H_4OMe); 133.3 (d, $J_{C,F}$ = 3.1, CH-6-C_6H_3F); 144.0 (d, $J_{C,F}$ = 7.9, C-4-C_6H_3F); 151.0 (C-7a-deazapurine); 152.2 (CH-2-deazapurine); 158.9 (C-4-deazapurine); 161.4 (C-*i*-C_6H_4OMe); 161.7 (d, $J_{C,F}$ = 244.9, C-2-C_6H_3F);.$^{19}F\{^1H\}$ NMR (470.3 MHz, CD_3OD): −113.1. MS (ESI^+): *m*/*z* (%) 451 (80) $[M + H]^+$, 473 (100) $[M + Na]^+$. HR-MS (ESI^+) for $C_{24}H_{24}O_4N_4F$: $[M + H]^+$ calculated 451.17761, found 451.17753. IR: 3613, 3568, 3522, 3410, 3203, 2984, 2933, 2872, 1614, 1571, 1543, 1496, 1469, 1453, 1391, 1381, 1372, 1355, 1259, 1230, 1145, 1104, 985, 949, 882.

5-[(3″-Fluoro-4‴-methoxy-[1″,1‴-biphenyl]-4″-yl)]-2′-deoxyuridine (dU^{BIF}). dU^{BIF} was prepared according to the general procedure, **dU^{I}** (26.5 mg, 0.075 mmol), **2a** (47 mg, 0.11 mmol). The product was isolated as white solid (20.8 mg, 65%). ^1H NMR (500.0 MHz, CD_3OD): 2.30 (ddd, 1H, J_{gem} = 13.6, $J_{2'b,1'}$ = 7.0, $J_{2'b,3'}$ = 6.1, H-2′b); 2.35 (ddd, 1H, J_{gem} = 13.6, $J_{2'a,1'}$ = 6.2, $J_{2'a,3'}$ = 3.8, H-2′a); 3.71, 3.78 (2 × dd, 2 × 1H, J_{gem} = 11.9, $J_{5',4'}$ = 3.3, H-5′); 3.83 (s, 3H, CH_3O); 3.95 (q, 1H, $J_{4',3'}$ = $J_{4',5'}$ = 3.3, H-4′); 4.42 (ddd, 1H, $J_{3',2'}$ = 6.1, 3.8, $J_{3',4'}$ = 3.3, H-3′); 6.35 (dd, 1H, $J_{1',2'}$ = 7.0, 6.2, H-1′); 7.01 (m, 2H, H-*m*-C_6H_4OMe); 7.36 (dd, 1H, $J_{H,F}$ = 11.8, $J_{3,5}$ = 1.7, H-3-C_6H_3F); 7.41 (dd, 1H, $J_{5,6}$ = 8.0, $J_{5,3}$ = 1.7, H-5-C_6H_3F); 7.46 (t, 1H, $J_{6,5}$ = $J_{H,F}$ = 8.0, H-6-C_6H_3F); 7.58 (m, 2H, H-*o*-C_6H_4OMe); 8.25 (d, 1H, $J_{H,F}$ = 0.8, H-6). ^{13}C NMR (125.7 MHz, CD_3OD): 41.7 (CH_2-2′); 55.8 (CH_3O); 62.6 (CH_2-5′); 72.2 (CH-3′); 86.8 (CH-1′); 89.0 (CH-4′); 110.8 (C-5); 114.3 (d, $J_{C,F}$ = 23.4, CH-3-C_6H_3F); 115.4 (CH-*m*-C_6H_4OMe); 119.9 (d, $J_{C,F}$ = 15.0, C-1-C_6H_3F); 123.0 (d, $J_{C,F}$ = 3.0, CH-5-C_6H_3F); 129.0 (CH-*o*-C_6H_4OMe); 133.0 (d, $J_{C,F}$ = 1.8, C-*i*-C_6H_4OMe); 133.1 (d, $J_{C,F}$ = 3.6, CH-6-C_6H_3F); 141.6 (d, $J_{C,F}$ = 2.8, CH-6); 144.2 (d, $J_{C,F}$ = 8.2, C-4-C_6H_3F); 151.9 (C-2); 161.32 (C-*p*-C_6H_4OMe); 162.0 (d, $J_{C,F}$ = 246.8, C-2-C_6H_3F); 164.17 (C-4). $^{19}F\{^1H\}$ NMR (470.3 MHz, CD_3OD): −112.1. MS (ESI^+): *m*/*z* (%) 429 (10) $[M + H]^+$, 451 (100) $[M + Na]^+$. HR-MS (ESI^+) for $C_{22}H_{22}O_6N_2F$: $[M + H]^+$ calculated 429.14564, found 429.14537. IR: 3434, 3057, 2924, 2842, 1682, 1622, 1610, 1498, 1462, 1428, 1402, 1296, 1277, 1248, 1180, 1095, 1050, 1028, 894, 825.

7-Deaza-7-[4″-(benzofuran-2‴-yl)-2″-fluorophenyl]-2′-deoxyadenosine (dA^{BFU}). dA^{BFU} was prepared according to the general procedure, **dA^{I}** (28.2 mg, 0.075 mmol), **2b** (136 mg, 0.11 mmol). The product was isolated as white solid (23 mg, 69%). ^1H NMR (500.0 MHz, CD_3OD): 2.37 (ddd, 1H, J_{gem} = 13.4, $J_{2'b,1'}$ = 6.1, $J_{2'b,3'}$ = 2.7, H-2′b); 2.72 (ddd, 1H, J_{gem} = 13.4, $J_{2'a,1'}$ = 8.2, $J_{2'a,3'}$ = 6.0, H-2′a); 3.74 (dd, 1H, J_{gem} = 12.1, $J_{5'b,4'}$ = 3.6, H-5′b); 3.82 (dd, 1H, J_{gem} = 12.1, $J_{5'a,4'}$ = 3.3, H-5′a); 4.04 (ddd, 1H, $J_{4',5'}$ = 3.6, 3.3, $J_{4',3'}$ = 2.5, H-4′); 4.55 (ddd, 1H, $J_{3',2'}$ = 6.0, 2.7, $J_{3',4'}$ = 2.5, H-3′); 6.59 (dd, 1H, $J_{1',2'}$ = 8.2, 6.1, H-1′); 7.24 (td, 1H, $J_{5,4}$ = $J_{5,6}$ = 7.3, $J_{5,7}$ = 1.0, H-5-benzofuryl); 7.28 (d, 1H, $J_{3,7}$ = 1.0, H-3-benzofuryl); 7.31 (ddd, 1H, $J_{6,7}$ = 8.3, $J_{6,5}$ = 7.3, $J_{6,4}$ = 1.3, H-6-benzofuryl); 7.51 (t, 1H, $J_{6,5}$ = $J_{H,F}$ = 8.0, H-6-C_6H_3F); 7.532 (d, 1H, $J_{H,F}$ = 0.8, H-6-deazapurine); 7.535 (dq, 1H, $J_{7,6}$ = 8.3, $J_{7,3}$ = $J_{7,4}$ = $J_{7,5}$ = 1.0, H-7-benzofuryl); 7.61 (ddd, 1H, $J_{4,5}$ = 7.3, $J_{4,6}$ = 1.3, $J_{4,7}$ = 1.0, H-4-benzofuryl); 7.75 (dd, 1H, $J_{H,F}$ = 10.9, $J_{3,5}$ = 1.7, H-3-C_6H_3F); 7.79 (dd, 1H, $J_{5,6}$ = 8.0, $J_{5,3}$ = 1.7, H-5-C_6H_3F); 8.15 (s, 1H, H-2-deazapurine). ^{13}C NMR (125.7 MHz, CD_3OD): 41.5 (CH_2-2′); 63.7 (CH_2-5′); 73.1 (CH-3′); 86.7 (CH-1′); 89.2 (CH-4′); 103.5 (C-4a-deazapurine); 104.0 (CH-3-benzofuryl); 110.6 (C-5-deazapurine); 112.1 (CH-7-benzofuryl); 113.2 (d, $J_{C,F}$ = 25.0, CH-3-C_6H_3F); 122.1 (d, $J_{C,F}$ = 3.3, CH-5-C_6H_3F); 122.3 (CH-4-benzofuryl); 123.0 (d, $J_{C,F}$ = 15.9, C-1-C_6H_3F); 124.4 (CH-5-benzofuryl); 124.4 (d, $J_{C,F}$ = 2.3, CH-6-deazapurine); 126.1 (CH-6-benzofuryl); 130.0 (C-3a-benzofuryl); 133.2 (d, $J_{C,F}$ = 8.5, C-4-C_6H_3F); 133.5 (d, $J_{C,F}$ = 3.0, CH-6-C_6H_3F); 151.1 (C-7a-deazapurine); 152.3 (CH-2-deazapurine); 155.4 (d, $J_{C,F}$ = 2.7, C-2-benzofuryl); 156.4 (C-7a-benzofuryl); 158.9 (C-4-deazapurine); 161.5 (d, $J_{C,F}$ = 245.4, C-2-C_6H_3F). $^{19}F\{^1H\}$ NMR (470.3 MHz, CD_3OD): −112.5. MS (ESI^+): *m*/*z* (%) 461 (100) $[M + H]^+$, 483 (90) $[M + Na]^+$. HR-MS (ESI^+) for $C_{25}H_{22}O_4N_4F$: $[M+H]^+$ calculated 461.1620, found 461.1619. IR: 3401, 2930, 2837, 1623, 1610, 1586, 1544, 1520, 1493, 1464, 1401, 1297, 1249, 1215, 1177, 1094, 1040, 1026, 992, 954, 926, 886, 825, 797.

5-[4″-(Benzofuran-2‴-yl)-2″-fluorophenyl]-2′-deoxyuridine (dU^{BFU}). dU^{BFU} was prepared according to the general procedure, **dU^{I}** (26.5 mg, 0.075 mmol), **2b** (136 mg, 0.11 mmol). The product was isolated as white solid (19 mg, 59%). ^1H NMR (600.1 MHz, CD_3OD): 2.32 (ddd, 1H, J_{gem} = 13.6, $J_{2'b,1'}$ = 7.0, $J_{2'b,3'}$ = 6.1, H-2′b); 2.36 (ddd, 1H, J_{gem} = 13.6, $J_{2'a,1'}$ = 6.2, $J_{2'a,3'}$ = 3.7, H-2′a); 3.72, 3.79 (2 × dd, 2 × 1H, J_{gem} = 11.9, $J_{5',4'}$ = 3.3, H-5′); 3.95 (q, 1H, $J_{4',3'}$ = $J_{4',5'}$ = 3.3, H-4′); 4.43 (ddd, 1H, $J_{3',2'}$ = 6.1, 3.7, $J_{3',4'}$ = 3.3, H-3′); 6.36 (dd, 1H, $J_{1',2'}$ = 7.0, 6.2, H-1′); 7.24 (ddd, 1H, $J_{5,4}$ = 7.7, $J_{5,6}$ = 7.2, $J_{5,7}$ = 1.0, H-5-benzofuryl); 7.28 (d, 1H, $J_{3,7}$ = 1.0, H-3-benzofuryl); 7.32 (ddd, 1H, $J_{6,7}$ = 8.3, $J_{6,5}$ = 7.2, $J_{6,4}$ = 1.3, H-6-benzofuryl); 7.54 (m, 2H, H-6-C_6H_3F, H-7-benzofuryl); 7.62 (ddd, 1H, $J_{4,5}$ = 7.7, $J_{4,6}$ = 1.3, $J_{4,7}$ = 0.7, H-4-benzofuryl); 7.68 (dd, 1H, $J_{H,F}$ = 11.2, $J_{3,5}$ = 1.7, H-3-C_6H_3F); 7.73 (dd, 1H, $J_{5,6}$ = 8.0, $J_{5,3}$ = 1.7, H-5-C_6H_3F); 8.31 (d, 1H, $J_{H,F}$ = 0.6, H-6). ^{13}C NMR (150.9 MHz, CD_3OD): 41.7 (CH_2-2′); 62.6 (CH_2-5′); 72.1 (CH-3′); 86.8 (CH-1′); 89.1 (CH-4′); 103.9 (CH-3-benzofuryl); 110.4 (C-5); 112.0 (CH-7-benzofuryl); 112.7 (d, $J_{C,F}$ = 25.2, CH-3-C_6H_3F); 121.4 (d, $J_{C,F}$ = 3.2, CH-5-C_6H_3F); 122.0 (d, $J_{C,F}$ = 15.0, C-1-C_6H_3F); 122.3 (CH-4-benzofuryl); 124.3 (CH-5-benzofuryl); 126.1 (CH-6-benzofuryl); 130.4 (C-3a-benzofuryl); 133.4 (d, $J_{C,F}$ = 3.2, CH-6-C_6H_3F); 133.5 (d, $J_{C,F}$ = 9.7, C-4-C_6H_3F); 141.9 (d, $J_{C,F}$ = 3.0, CH-6); 151.8 (C-2); 155.5 (d, $J_{C,F}$ = 2.7, C-2-benzofuryl); 156.4 (C-7a-benzofuryl); 161.9 (d, $J_{C,F}$ = 247.2, C-2-C_6H_3F); 164.0 (C-4). $^{19}F\{^1H\}$ NMR (470.3 MHz, CD_3OD): −111.5. MS (ESI^+): *m*/*z* (%) 461 (100) $[M + Na]^+$. HR-MS (ESI^+) for $C_{23}H_{19}O_6N_2FNa$: $[M + Na]^+$ calculated 461.1119, found 461.1119. IR: 3435, 3163, 3039, 2921, 1692, 1667, 1626, 1501, 1465, 1451, 1430, 1300, 1282, 1259, 1111, 1083, 1066, 926, 945, 889, 804, 752.

7-Deaza-7-[4″-(benzo[*d*]oxazol-2‴-yl)-2″-fluorophenyl]-2′-deoxyadenosine (dA^{BOX}). dA^{BOX} was prepared according to the general procedure, **dA^{I}** (28.2 mg, 0.075 mmol), **2c** (55.3 mg, 0.11 mmol). The product was isolated as white solid (19 mg, 57%). ^1H NMR (500.0 MHz, DMSO-d_6): 2.23 (ddd, 1H, J_{gem} = 13.1, $J_{2'b,1'}$ = 5.9, $J_{2'b,3'}$ = 2.7, H-2′b); 2.57 (ddd, 1H, J_{gem} = 13.1, $J_{2'a,1'}$ = 8.1, $J_{2'a,3'}$ = 5.8, H-2′a); 3.52 (ddd, 1H, J_{gem} = 11.8, $J_{5'b,OH}$ = 5.9, $J_{5'b,4'}$ = 4.4, H-5′b); 3.59 (ddd, 1H, J_{gem} = 11.8, $J_{5'a,OH}$ = 5.1, $J_{5'a,4'}$ = 4.4, H-5′b); 3.85 (td, 1H, $J_{4',5'}$ = 4.4, $J_{4',3'}$ = 2.4, H-4′); 4.37 (m, 1H, $J_{3',2'}$ = 5.8, 2.7, $J_{3',OH}$ = 4.0, $J_{3',4'}$ = 2.4, H-3′); 5.07 (dd, 1H, $J_{OH,5'}$ = 5.9, 5.1, OH-5′); 5.29 (d, 1H, $J_{OH,3'}$ = 4.0, OH-3′); 6.33 (bs, 2H, NH_2-deazapurine); 6.61 (dd, 1H, $J_{1',2'}$ = 8.1, 5.9, H-1′); 7.45 (td, 1H, $J_{5,4}$ = $J_{5,6}$ = 7.4, $J_{5,7}$ = 1.4, H-5-benzoxazole); 7.48 (td, 1H, $J_{6,5}$ = $J_{6,7}$ = 7.4, $J_{6,4}$ = 1.5, H-6-benzoxazole); 7.66 (t, 1H, $J_{6,5}$ = $J_{H,F}$ = 8.0, H-6-C_6H_3F); 7.70 (d, 1H, $J_{H,F}$ = 0.9, H-6-deazapurine); 7.84 (ddd, 1H, $J_{7,6}$ = 7.4, $J_{7,5}$ = 1.4, $J_{7,4}$ = 0.6, H-7-benzoxazole); 7.86 (ddd, 1H, $J_{4,5}$ = 7.4, $J_{4,6}$ = 1.5, $J_{4,7}$ = 0.6, H-4-benzoxazole); 8.06 (dd, 1H, $J_{H,F}$ = 10.5, $J_{3,5}$ = 1.7, H-3-C_6H_3F); 8.12 (dd, 1H, $J_{5,6}$ = 8.0, $J_{5,3}$ = 1.7, H-5-C_6H_3F); 8.17 (s, 1H, H-2-deazapurine). ^{13}C NMR (125.7 MHz, DMSO-d_6): 39.7 (CH_2-2′); 62.2 (CH_2-5′); 71.3 (CH-3′); 83.4 (CH-1′); 87.7 (CH-4′); 101.1 (C-4a-deazapurine); 108.4 (C-5-deazapurine); 111.3 (CH-7-benzoxazole); 114.8 (d, $J_{C,F}$ = 25.1, CH-3-C_6H_3F); 120.2 (CH-4-benzoxazole); 122.9 (d, $J_{C,F}$ = 2.4, CH-6-deazapurine); 123.8 (d, $J_{C,F}$ = 2.6, CH-5-C_6H_3F); 125.3 (CH-5-benzoxazole); 125.9 (d, $J_{C,F}$ = 15.7, C-1-C_6H_3F); 126.1 (CH-6-benzoxazole); 126.9 (d, $J_{C,F}$ = 8.6, C-4-C_6H_3F); 132.9 (d, $J_{C,F}$ = 3.3, CH-6-C_6H_3F); 141.6 (C-3a-benzoxazole); 150.5 (C-7a-benzoxazole); 150.7 (C-7a-deazapurine); 152.1 (CH-2-deazapurine); 157.6 (C-4-deazapurine); 159.6 (d, $J_{C,F}$ = 245.4, C-2-C_6H_3F); 161.4 (d, $J_{C,F}$ = 2.8, C-2-benzoxazole). $^{19}F\{^1H\}$ NMR (470.3 MHz, DMSO-d_6): −110.9. MS (ESI^+): *m*/*z* (%) 462 (60) $[M + H]^+$, 484 (100) $[M + Na]^+$. HR-MS (ESI^+) for $C_{24}H_{21}O_4N_5F$: $[M + H]^+$ calculated 462.1572, found 462.1572. IR: 3405, 2923, 2854, 2360, 2342, 1700, 1626, 1589, 1536, 1454, 1373, 1348, 1305, 1243, 1219, 1178, 1095, 1058, 1002, 961, 883, 796, 761, 747.

5-[4″-(Benzo[*d*]oxazol-2‴-yl)-2″-fluorophenyl]-2′-deoxyuridine (dU^{BOX}). dU^{BOX} was prepared according to the general procedure, **dU^{I}** (26.5 mg, 0.075 mmol), **2c** (55.3 mg, 0.11 mmol). The product was isolated as white solid (23 mg, 71%). ^1H NMR (500.0 MHz, DMSO-d_6): 2.18 (ddd, 1H, J_{gem} = 13.4, $J_{2'b,1'}$ = 6.2, $J_{2'b,3'}$ = 3.9, H-2′b); 2.22 (ddd, 1H, J_{gem} = 13.4, $J_{2'a,1'}$ = 7.0, $J_{2'a,3'}$ = 5.8, H-2′a); 3.54, 3.59 (2 × ddd, 2 × 1H, J_{gem} = 11.8, $J_{5',OH}$ = 5.0, $J_{5',4'}$ = 3.5, H-5′b); 3.81 (q, 1H, $J_{4',3'}$ = $J_{4',5'}$ = 3.5, H-4′); 4.27 (m, 1H, $J_{3',2'}$ = 5.8, 3.9, $J_{3',OH}$ = 4.3, $J_{3',4'}$ = 3.5, H-3′); 5.02 (t, 1H, $J_{OH,5'}$ = 5.0, OH-5′); 5.27 (d, 1H, $J_{OH,3'}$ = 4.3, OH-3′); 6.24 (dd, 1H, $J_{1',2'}$ = 7.0, 6.2, H-1′); 7.44 (td, 1H,

dx.doi.org/10.1021/jo202321g | J. Org. Chem. 2012, 77, 1026−1044

$J_{5,4} = J_{5,6}$ = 7.4, $J_{5,7}$ = 1.4, H-5-benzoxazole); 7.48 (td, 1H, $J_{6,5} = J_{6,7}$ = 7.4, $J_{6,4}$ = 1.5, H-6-benzoxazole); 7.66 (dd, 1H, $J_{6,5}$ =8.0, $J_{H,F}$ = 7.6, H-6-C_6H_3F); 7.82 (ddd, 1H, $J_{7,6}$ = 7.4, $J_{7,5}$ = 1.4, $J_{7,4}$ = 0.6, H-7-benzoxazole); 7.85 (ddd, 1H, $J_{4,5}$ = 7.4, $J_{4,6}$ = 1.5, $J_{4,7}$ = 0.6, H-4-benzoxazole); 7.98 (dd, 1H, $J_{H,F}$ = 10.6, $J_{3,5}$ = 1.7, H-3-C_6H_3F); 8.05 (dd, 1H, $J_{5,6}$ = 8.0, $J_{5,3}$ = 1.7, H-5-C_6H_3F); 8.27 (s, 1H, H-6); 11.68 (bs, 1H, NH). ^{13}C NMR (125.7 MHz, DMSO-d_6): 40.2 (CH_2-2′); 61.2 (CH_2-5′); 70.4 (CH-3′); 84.8 (CH-1′); 87.8 (CH-4′); 108.0 (C-5); 111.3 (CH-7-benzoxazole); 114.3 (d, $J_{C,F}$ = 25.3, CH-3-C_6H_3F); 120.2 (CH-4-benzoxazole); 123.2 (d, $J_{C,F}$ = 3.2, CH-5-C_6H_3F); 124.8 (d, $J_{C,F}$ = 14.7, C-1-C_6H_3F); 125.3 (CH-5-benzoxazole); 126.1 (CH-6-benzoxazole); 127.7 (d, $J_{C,F}$ = 8.8, C-4-C_6H_3F); 133.1 (d, $J_{C,F}$ = 3.5, CH-6-C_6H_3F); 140.8 (d, $J_{C,F}$ = 2.8, CH-6); 141.6 (C-3a-benzoxazole); 150.1 (C-2); 150.50 (C-7a-benzoxazole); 159.9 (d, $J_{C,F}$ = 248.2, C-2-C_6H_3F); 161.2 (d, $J_{C,F}$ = 2.9, C-2-benzoxazole); 161.4 (C-4). ^{19}F{^{1}H} NMR (470.3 MHz, DMSO-d_6): −108.9. MS (ESI$^+$): m/z (%) 462 (100) [M + Na]$^+$. HR-MS (ESI$^+$) for $C_{22}H_{18}O_6N_3FNa$: [M+Na]$^+$ calculated 462.10718, found 462.10716. IR: 3445, 3064, 1718, 1687, 1628, 1556, 1501, 1455, 1426, 1414, 1293, 1243, 1213, 1098, 1062, 1003, 955, 884, 761, 746.

7-Deaza-7-[4″-(5‴-aminobenzo[*d*]oxazol-2‴-yl)-2″-fluorophenyl]-2′-deoxyadenosine (dA^{ABOX}). **dA^{ABOX}** was prepared according to the general procedure, **dA^{I}** (28.2 mg, 0.075 mmol), **2d** (74 mg, 0.11 mmol). The product was isolated as yellow solid (18 mg, 44%). ^{1}H NMR (500.0 MHz, DMSO-d_6): 2.23 (ddd, 1H, J_{gem} = 13.2, $J_{2'b,1'}$ = 6.0, $J_{2'b,3'}$ = 2.7, H-2′b); 2.56 (ddd, 1H, J_{gem} = 13.2, $J_{2'a,1'}$ = 8.2, $J_{2'a,3'}$ = 5.9, H-2′a); 3.52 (ddd, 1H, J_{gem} = 11.7, $J_{5'b,OH}$ = 5.9, $J_{5'b,4'}$ = 4.3, H-5′b); 3.59 (ddd, 1H, J_{gem} = 11.7, $J_{5'a,OH}$ = 5.2, $J_{5'a,4'}$ = 4.3, H-5′b); 3.85 (td, 1H, $J_{4',5'}$ = 4.3, $J_{4',3'}$ = 2.5, H-4′); 4.37 (m, 1H, $J_{3',2'}$ = 5.9, 2.7, $J_{3',OH}$ = 4.1, $J_{3',4'}$ = 2.5, H-3′); 5.07 (dd, 1H, $J_{OH,5'}$ = 5.9, 5.2, OH-5′); 5.16 (bs, 2H, NH_2-benzoxazole); 5.28 (d, 1H, $J_{OH,3'}$ = 4.1, OH-3′); 6.30 (bs, 2H, NH_2-deazapurine); 6.60 (dd, 1H, $J_{1',2'}$ = 8.2, 6.0, H-1′); 6.70 (dd, 1H, $J_{6,7}$ = 8.7, $J_{6,4}$ = 2.3, H-6-benzoxazole); 6.90 (d, 1H, $J_{4,5}$ = 2.3, H-4-benzoxazole); 7.45 (d, 1H, $J_{7,6}$ = 8.7, H-7-benzoxazole); 7.61 (t, 1H, $J_{6,5} = J_{H,F}$ = 8.0, H-6-C_6H_3F); 7.68 (d, 1H, $J_{H,F}$ = 0.8, H-6-deazapurine); 7.97 (dd, 1H, $J_{H,F}$ = 10.6, $J_{3,5}$ = 1.7, H-3-C_6H_3F); 8.03 (dd, 1H, $J_{5,6}$ = 8.0, $J_{5,3}$ = 1.7, H-5-C_6H_3F); 8.16 (s, 1H, H-2-deazapurine). ^{13}C NMR (125.7 MHz, DMSO-d_6): 39.7 (CH_2-2′); 62.2 (CH_2-5′); 71.3 (CH-3′); 83.3 (CH-1′); 87.7 (CH-4′); 101.1 (C-4a-deazapurine); 102.7 (CH-4-benzoxazole); 108.4 (C-5-deazapurine); 110.8 (CH-7-benzoxazole); 113.8 (CH-6-benzoxazole); 114.4 (d, $J_{C,F}$ = 25.1, CH-3-C_6H_3F); 122.8 (d, $J_{C,F}$ = 3.0, CH-6-deazapurine); 123.4 (d, $J_{C,F}$ = 2.8, CH-5-C_6H_3F); 125.2 (d, $J_{C,F}$ = 15.5, C-1-C_6H_3F); 127.4 (d, $J_{C,F}$ = 8.6, C-4-C_6H_3F); 132.8 (d, $J_{C,F}$ = 2.9, CH-6-C_6H_3F); 142.7 (C-3a-benzoxazole); 142.9 (C-7a-benzoxazole); 147.1 (C-5-benzoxazole); 150.7 (C-7a-deazapurine); 152.1 (CH-2-deazapurine); 157.6 (C-4-deazapurine); 159.6 (d, $J_{C,F}$ = 245.1, C-2-C_6H_3F); 161.0 (d, $J_{C,F}$ = 3.0, C-2-benzoxazole). ^{19}F{^{1}H} NMR (470.3 MHz, DMSO-d_6): −111.1. MS (ESI$^+$): m/z (%) 477 (80) [M + H]$^+$, 499 (100) [M + Na] $^+$. HR-MS (ESI$^+$) for $C_{24}H_{22}O_4N_6F$: [M + H]$^+$ calculated 477.16811, found 477.16810. IR: 3411, 2922, 2855, 1627, 1590, 1534, 1487, 1468, 1450, 1352, 1306, 1217, 1182, 1094, 1057, 993, 884, 798.

5-[4″-(5‴-Aminobenzo[*d*]oxazol-2‴-yl)-2″-fluorophenyl]-2′-deoxyuridine (dU^{ABOX}). **dU^{ABOX}** was prepared according to the general procedure, **dU^{I}** (26.5 mg, 0.075 mmol), **2d** (74 mg, 0.11 mmol). The product was isolated as yellow solid (21 mg, 61%). ^{1}H NMR (500.0 MHz, DMSO-d_6): 2.18 (ddd, 1H, J_{gem} = 13.2, $J_{2'b,1'}$ = 6.2, $J_{2'b,3'}$ = 3.8, H-2′b); 2.21 (ddd, 1H, J_{gem} = 13.2, $J_{2'a,1'}$ = 7.0, $J_{2'a,3'}$ = 5.9, H-2′a); 3.54, 3.59 (2 × dd, 2 × 1H, J_{gem} = 12.2, $J_{5',4'}$ = 3.5, H-5′); 3.81 (q, 1H, $J_{4',3'} = J_{4',5'}$ = 3.5, H-4′); 4.27 (ddd, 1H, $J_{3',2'}$ = 5.9, 3.8, $J_{3',4'}$ = 3.5, H-3′); 5.02 (bs, 1H, OH-5′); 5.16 (bs, 2H, NH_2-benzoxazole); 5.27 (bs, 1H, OH-3′); 6.23 (dd, 1H, $J_{1',2'}$ = 7.0, 6.2, H-1′); 6.70 (dd, 1H, $J_{6,7}$ = 8.7, $J_{6,4}$ = 2.3, H-6-benzoxazole); 6.89 (dd, 1H, $J_{4,6}$ = 2.3, $J_{4,7}$ = 0.5, H-4-benzoxazole); 7.44 (dd, 1H, $J_{7,6}$ = 8.7, $J_{7,4}$ = 0.5, H-7-benzoxazole); 7.65 (dd, 1H, $J_{6,5}$ = 8.1, $J_{H,F}$ = 7.5, H-6-C_6H_3F); 7.89 (dd, 1H, $J_{H,F}$ = 10.7, $J_{3,5}$ = 1.7, H-3-C_6H_3F); 7.97 (dd, 1H, $J_{5,6}$ = 8.1, $J_{5,3}$ = 1.7, H-5-C_6H_3F); 8.25 (s, 1H, H-6); 11.66 (bs, 1H, NH). ^{13}C NMR (125.7 MHz, DMSO-d_6): 40.2 (CH_2-2′); 61.2 (CH_2-5′); 70.4 (CH-3′); 84.8 (CH-1′); 87.7 (CH-4′); 102.7 (CH-4-benzoxazole); 108.1 (C-5); 110.9 (CH-7-benzoxazole); 113.8 (d, $J_{C,F}$ = 25.3, CH-3-C_6H_3F); 113.9 (CH-6-bezoxazole); 122.7 (d, $J_{C,F}$ = 3.1, CH-5-C_6H_3F); 124.2 (d, $J_{C,F}$ = 14.6, C-1-C_6H_3F); 127.2 (d, $J_{C,F}$ = 8.6, C-4-C_6H_3F); 132.9 (d, $J_{C,F}$ = 3.3, CH-6-C_6H_3F); 140.7 (d, $J_{C,F}$ = 2.6, CH-6); 142.6 (C-3a-benzoxazole); 142.9 (C-7a-benzoxazole); 147.1 (C-5-benzoxazole); 150.1 (C-2); 159.9 (d, $J_{C,F}$ = 247.8, C-2-C_6H_3F); 160.8 (d, $J_{C,F}$ = 3.1, C-2-benzoxazole); 161.4 (C-4). ^{19}F{^{1}H} NMR (470.3 MHz, DMSO-d_6): −113.0. MS (ESI$^+$): m/z (%) 455 (100) [M + H]$^+$, 477 (31) [M + Na]$^+$. HR-MS (ESI$^+$) for $C_{22}H_{20}O_6N_4F$: [M + H]$^+$ calculated 455.1361, found 455.1360. IR: 3421, 3064, 1704, 1628, 1574, 1551, 1490, 1451, 1416, 1354, 1315, 1299, 1209, 1185, 1101, 1091, 1060, 961, 890, 808, 782.

General Procedure for Suzuki Cross-Coupling of Base-Halogenated Nucleoside Triphosphates Analogues (dN^{I}TPs) with Biaryl Pinacolatoboronates. A mixture of H_2O/CH_3CN (2:1, 2 mL) was added to an argon-purged flask containing nucleoside analogue **dN^{I}TP** (0.05 mmol), a biaryl pinacolatoboronate (0.075 mmol, 1.5 equiv), and Cs_2CO_3 (49 mg, 0.15 mmol, 3 equiv). In a separate flask, $Pd(OAc)_2$ (0.56 mg, 0.0025 mmol, 5 mol %) and $P(Ph\text{-}SO_3Na)_3$ (3.59 mg, 0.00625 mmol, 2.5 equiv. to Pd) were combined, and the flask was evacuated and purged with argon followed by addition of H_2O/CH_3CN (2:1, 0.5 mL). The mixture of catalyst was then injected to the reaction mixture, and the reaction mixture was stirred at 90 °C for 0.75 h. The products were isolated by C18 reverse phase column chromatogryphy using water/methanol (5−100%) as eluent.

7-Deaza-7-[(3″-fluoro-4‴-methoxy-[1″,1‴-biphenyl]-4″-yl)]-2′-deoxyadenosine 5′-*O*-Triphosphate (dA^{BIF}TP). **dA^{BIF}TP** was prepared according to the general procedure, **dA^{I}TP** (35.2 mg, 0.05 mmol), **2a** (33 mg, 0.075 mmol). The product was isolated as white solid (8.5 mg, 22%). ^{1}H NMR (499.8 MHz, D_2O, pD = 7.1, phosphate buffer): 2.36 (ddd, 1H, J_{gem} = 13.9, $J_{2'b,1'}$ = 6.1, $J_{2'b,3'}$ = 3.0, H-2′b); 2.61 (ddd, 1H, J_{gem} = 13.9, $J_{2'a,1'}$ = 8.1, $J_{2'a,3'}$ = 6.3, H-2′a); 3.81 (s, 3H, CH_3O); 4.10, 4.15 (2 × ddd, 2 × 1H, J_{gem} = 11.2, $J_{H,P}$ = 6.4, $J_{5',4'}$ = 4.9, H-5′); 4.23 (td, 1H, $J_{4',5'}$ = 4.9, $J_{4',3'}$ = 2.2, H-4′); 4.69 (ddd, 1H, $J_{3',2'}$ = 6.3, 3.0, $J_{3',4'}$ = 2.2, H-3′); 6.53 (dd, 1H, $J_{1',2'}$ = 8.1, 6.1, H-1′); 6.86 (m, 2H, H-*m*-C_6H_4OMe); 7.26 (t, 1H, $J_{6,5} = J_{H,F}$ = 8.2, H-6-C_6H_3F); 7.28 (s, 1H, H-6-deazapurine); 7.29 (d, 1H, $J_{H,F}$ = 11.0, H-3-C_6H_3F); 7.42 (m, 3H, H-5-C_6H_3F, H-*o*-C_6H_4OMe); 8.11 (s, 1H, H-2-deazapurine). ^{13}C NMR (125.7 MHz, D_2O, pD = 7.1, phosphate buffer): 40.9 (CH_2-2′); 58.0 (CH_3O); 68.3 (d, $J_{C,P}$ = 5.1, CH_2-5′); 73.8 (CH-3′); 85.5 (CH-1′); 87.7 (d, $J_{C,P}$ = 8.8, CH-4′); 104.4 (C-4a-deazapurine); 113.1 (C-5-deazapurine); 116.2 (d, $J_{C,F}$ = 23.4, CH-3-C_6H_3F); 116.9 (CH-*m*-C_6H_4OMe); 121.6 (d, $J_{C,F}$ = 15.1, C-1-C_6H_3F); 124.2 (CH-5-C_6H_3F); 125.1 (CH-6-deazapurine); 130.5 (CH-*o*-C_6H_4OMe); 134.0 (C-*i*-C_6H_4OMe); 134.5 (CH-6-C_6H_3F); 144.2 (d, $J_{C,F}$ = 9.1, C-4-C_6H_3F); 152.3 (C-7a-deazapurine); 153.7 (CH-2-deazapurine); 159.6 (C-4-deazapurine); 161.5 (C-*p*-C_6H_4OMe); 162.4 (d, $J_{C,F}$ = 244.4, C-2-C_6H_3F). ^{31}P{^{1}H} NMR (202.3 MHz, D_2O, pD = 7.1, phosphate buffer, ref(phosphate buffer) = 2.35 ppm): −20.95 (bdd, J = 18.6, 17.1, P_β); −10.32 (d, J = 18.6, P_α); −6.27 (bd, J = 17.1, P_γ). ^{19}F{^{1}H} NMR (470.3 MHz, D_2O, pD = 7.1, phosphate buffer): −112.3. MS (ESI$^-$): m/z (%) 609.1 (100) [M$^-$ + 2H-PO_3H], 631.1 (40) [M + H + Na - PO_3H]$^-$, 689.1 (10) [M + 2H]$^-$, 711.0 (20) [M + H + Na]$^-$. HR-MS (ESI$^-$) for $C_{24}H_{25}O_{13}N_4FP_3$: [M + 2H]$^-$ calculated 689.0620, found 689.0618.

5-[(3″-Fluoro-4‴-methoxy-[1″,1‴-biphenyl]-4″-yl)]-2′-deoxyuridine 5′-*O*-Triphosphate (dU^{BIF}TP). **dU^{BIF}TP** was prepared according to the general procedure, **dU^{I}TP** (34 mg, 0.05 mmol), **2a** (33 mg, 0.075 mmol). The product was isolated as white solid (7.9 mg, 21%). ^{1}H NMR (499.8 MHz, D_2O, pD = 7.1, phosphate buffer, ref(dioxane) = 3.75 ppm): 2.42 (ddd, 1H, J_{gem} = 14.2, $J_{2'b,1'}$ = 6.6, $J_{2'b,3'}$ = 4.1, H-2′b); 2.46 (ddd, 1H, J_{gem} = 14.2, $J_{2'a,1'}$ = 7.3, $J_{2'a,3'}$ = 5.9, H-2′a); 3.89 (s, 3H, CH_3O); 4.17 (bm, 2H, H-5′); 4.22 (bm, 1H, H-4′); 4.64 (dt, 1H, $J_{3',2'}$ = 5.9, 4.1, $J_{3',4'}$ = 4.1, H-3′); 6.35 (dd, 1H, $J_{1',2'}$ = 7.3, 6.6, H-1′); 7.12 (m, 2H, H-*m*-C_6H_4OMe); 7.47 (t, 1H, $J_{6,5} = J_{H,F}$ = 7.8, H-6-C_6H_3F); 7.46 (dd, 1H, $J_{H,F}$ = 11.7, $J_{3,5}$ = 1.8, H-3-C_6H_3F); 7.54 (dd, 1H, $J_{5,6}$ = 8.0, $J_{5,3}$ = 1.8, H-5-C_6H_3F); 7.72 (m, 2H, H-*o*-C_6H_4OMe); 7.93 (s, 1H, H-6). ^{13}C NMR (125.7 MHz, D_2O, pD = 7.1, phosphate buffer, ref(dioxane) = 69.3 ppm): 41.1 (CH_2-2′); 58.2 (CH_3O); 68.1 (d, $J_{C,P}$ = 5.7, CH_2-5′); 73.4 (CH-3′); 88.3 (d, $J_{C,P}$ = 8.9, CH-4′);

dx.doi.org/10.1021/jo202321g | J. Org. Chem. 2012, 77, 1026−1044

88.4 (CH-1′); 113.5 (C-5); 116.1 (d, $J_{C,F}$ = 23.0, CH-3-C_6H_3F); 117.3 (CH-*m*-C_6H_4OMe); 120.4 (d, $J_{C,F}$ = 15.7, C-1-C_6H_3F); 125.2 (d, $J_{C,F}$ = 3.2, CH-5-C_6H_3F); 131.0 (CH-*o*-C_6H_4OMe); 134.6 (d, $J_{C,F}$ = 1.8, C-*i*-C_6H_4OMe); 134.8 (d, $J_{C,F}$ = 3.1, CH-6-C_6H_3F); 143.2 (CH-6); 145.5 (d, $J_{C,F}$ = 8.5, C-4-C_6H_3F); 154.1 (C-2); 161.8 (C-*p*-C_6H_4OMe); 163.2 (d, $J_{C,F}$ = 246.0, C-2-C_6H_3F); 167.2 (C-4). $^{31}P\{^1H\}$ NMR (202.3 MHz, D_2O, pD = 7.1, phosphate buffer): −21.47 (bdd, *J* = 21.0, 19.5, P_β); −10.56 (d, *J* = 19.5, P_α); −6.86 (bd, *J* = 21.0, P_γ). $^{19}F\{^1H\}$ NMR (470.3 MHz, D_2O, pD = 7.1, phosphate buffer): −110.6. MS (ESI⁻): *m*/*z* (%) 587.1 (100) [M + 2H - PO_3H]⁻, 609.1 (30) [M + H + Na -PO_3H]⁻, 667.1 (5) [M + 2H]⁻, 689.1 (13) [M + H + Na]⁻. HR-MS (ESI⁻) for $C_{22}H_{23}O_{15}N_2FP_3$: [M + 2H]⁻ calculated 667.0301, found 667.0291.

7-Deaza-7-[4″-(benzofuran-2‴-yl)-2″-fluorophenyl]-2′-deoxyadenosine 5′-*O*-Triphosphate (dA^{BFU}TP). dA^{BFU}TP was prepared according to the general procedure, **dA^{I}TP** (35.2 mg, 0.05 mmol), **2b** (92 mg, 0.075 mmol). The product was isolated as white solid (11 mg, 28%). ^1H NMR (499.8 MHz, D_2O, pD = 7.1, phosphate buffer, ref(dioxane) = 3.75 ppm): 2.42 (ddd, 1H, J_{gem} = 13.8, $J_{2'b,1'}$ = 5.7, $J_{2'b,3'}$ = 2.9, H-2′b); 2.65 (dt, 1H, J_{gem} = 13.8, $J_{2'a,1'}$ = $J_{2'a,3'}$ = 7.3, H-2′a); 4.08 (ddd, 1H, J_{gem} = 11.3, $J_{H,P}$ = 5.0, $J_{5'b,4'}$ = 4.2, H-5′b); 4.12 (ddd, 1H, J_{gem} = 11.3, $J_{H,P}$ = 6.4, $J_{5'a,4'}$ = 4.2, H-5′a); 4.21 (q, 1H, $J_{4',5'}$ = $J_{4',3'}$ = 4.2, H-4′); 4.71 (bm, 1H, H-3′); 6.40 (dd, 1H, $J_{1',2'}$ = 7.3, 5.7, H-1′); 7.02 (s, 1H, H-3-benzofuryl); 7.19 (t, 1H, $J_{5,4}$ = $J_{5,6}$ = 7.1, H-5-benzofuryl); 7.26 (t, 1H, $J_{6,7}$ = $J_{6,5}$ = 7.1, H-6-benzofuryl); 7.34 (m, 2H, H-6-C_6H_3F, H-7-benzofuryl); 7.44 (d, 1H, $J_{4,5}$ = 7.1, H-4-benzofuryl); 7.45 (s, 1H, H-6-deazapurine); 7.56 (d, 1H, $J_{5,6}$ = 8.0, H-5-C_6H_3F); 7.59 (d, 1H, $J_{H,F}$ = 11.0, H-3-C_6H_3F); 7.98 (s, 1H, H-2-deazapurine). ^{13}C NMR (125.7 MHz, D_2O, pD = 7.1, phosphate buffer, ref(dioxane) = 69.3 ppm): 40.9 (CH_2-2′); 68.28 (d, $J_{C,P}$ = 6.2, CH_2-5′); 73.8 (CH-3′); 85.4 (CH-1′); 87.7 (d, $J_{C,P}$ = 8.6, CH-4′); 104.1 (C-4a-deazapurine); 105.6 (CH-3-benzofuryl); 112.8 (C-5-deazapurine); 113.5 (CH-7-benzofuryl); 114.9 (d, $J_{C,F}$ = 25.9, CH-3-C_6H_3F); 123.4 (d, $J_{C,F}$ = 14.7, C-1-C_6H_3F); 123.6 (CH-5-C_6H_3F); 123.8 (CH-4-benzofuryl); 124.3 (CH-6-deazapurine); 125.9 (CH-5-benzofuryl); 127.6 (CH-6-benzofuryl); 131.2 (C-3a-benzofuryl); 133.7 (d, $J_{C,F}$ = 8.7, C-4-C_6H_3F); 134.6 (CH-6-C_6H_3F); 152.1 (C-7a-deazapurine); 153.5 (CH-2-deazapurine); 156.3 (d, $J_{C,F}$ = 2.9, C-2-benzofuryl); 157.0 (C-7a-benzofuryl); 159.4 (C-4-deazapurine); 162.1 (d, $J_{C,F}$ = 242.6, C-2-C_6H_3F). $^{31}P\{^1H\}$ NMR (202.3 MHz, D_2O, pD = 7.1, phosphate buffer, ref(phosphate buffer) = 2.35 ppm): −21.30 (dd, *J* = 20.3, 19.0, P_β); −10.21 (d, *J* = 19.0, P_α); −6.86 (bd, *J* = 20.3, P_γ). $^{19}F\{^1H\}$ NMR (470.3 MHz, D_2O, pD = 7.1, phosphate buffer): −111.7. MS (ESI⁻): *m*/*z* (%) 619.1 (100) [M + 2H - PO_3H]⁻, 641.1 (30) [M + H + Na - PO_3H]⁻, 699.0 (20) [M + 2H]⁻, 721.0 (20) [M + H + Na]⁻. HR-MS (ESI⁻) for $C_{25}H_{23}O_{13}N_4FP_3$: [M + 2H]⁻ calculated 699.0464, found 699.0463.

5-[4″-(Benzofuran-2‴-yl)-2″-fluorophenyl]-2′-deoxyuridine 5′-*O*-Triphosphate (dU^{BFU}TP). dU^{BFU}TP was prepared according to the general procedure, **dU^{I}TP** (34 mg, 0.05 mmol), **2b** (92 mg, 0.075 mmol). The product was isolated as white solid (7.2 mg, 17%). ^1H NMR (499.8 MHz, D_2O, pD = 7.1, phosphate buffer, ref(dioxane) = 3.75 ppm): 2.44 (m, 2H, H-2′); 4.18 (m, 2H, H-5′); 4.21 (m, 1H, H-4′); 4.64 (m, 1H, H-3′); 6.33 (t, 1H, $J_{1',2'}$ = 6.9, H-1′); 7.32 (t, 1H, $J_{5,4}$ = $J_{5,6}$ = 7.3, H-5-benzofuryl); 7.33 (s, 1H, H-3-benzofuryl); 7.39 (ddd, 1H, $J_{6,7}$ = 8.2, $J_{6,5}$ = 7.3, $J_{6,4}$ = 1.1, H-6-benzofuryl); 7.52 (t, 1H, $J_{H,F}$ = $J_{6,5}$ = 7.8, H-6-C_6H_3F); 7.62 (d, 1H, $J_{7,6}$ = 8.2, H-7-benzofuryl); 7.71 (d, 1H, $J_{4,5}$ = 7.3, H-4-benzofuryl); 7.72 (dd, 1H, $J_{H,F}$ = 11.0, $J_{3,5}$ = 1.6, H-3-C_6H_3F); 7.79 (dd, 1H, $J_{5,6}$ = 7.8, $J_{5,3}$ = 1.6, H-5-C_6H_3F); 7.95 (s, 1H, H-6). ^{13}C NMR (125.7 MHz, D_2O, pD = 7.1, phosphate buffer, ref(dioxane) = 69.3 ppm): 41.2 (CH_2-2′); 68.1 (d, $J_{C,P}$ = 4.2, CH_2-5′); 73.4 (CH-3′); 88.3 (d, $J_{C,P}$ = 8.8, CH-4′); 88.43 (CH-1′); 105.9 (CH-3-benzofuryl); 113.2 (C-5); 114.0 (CH-7-benzofuryl); 114.5 (d, $J_{C,F}$ = 25.0, CH-3-C_6H_3F); 122.2 (d, $J_{C,F}$ = 16.4, C-1-C_6H_3F); 123.6 (CH-5-C_6H_3F); 124.2 (CH-4-benzofuryl); 126.1 (CH-5-benzofuryl); 127.8 (CH-6-benzofuryl); 131.6 (C-3a-benzofuryl); 135.0 (CH-6-C_6H_3F); 135.1 (d, $J_{C,F}$ = 9.0, C-4-C_6H_3F); 143.4 (CH-6); 154.0 (C-2); 156.9 (C-2-benzofuryl); 157.4 (C-7a-benzofuryl); 163.0 (d, $J_{C,F}$ = 245.8, C-2-C_6H_3F); 167.0 (C-4). $^{31}P\{^1H\}$ NMR (202.3 MHz, D_2O, pD = 7.1, phosphate buffer, ref(phosphate buffer) = 2.35 ppm): −21.49 (t, *J* = 19.5, P_β); −10.60 (d, *J* = 19.5, P_α); −6.87 (bd, *J* = 19.5, P_γ). $^{19}F\{^1H\}$ NMR (470.3 MHz, D_2O, pD = 7.1, phosphate buffer): −110.1. MS (ESI⁻): *m*/*z* (%) 597.1 (90) [M + 2H - PO_3H]⁻, 619.1 (35) [M + H + Na - PO_3H]⁻, 677.1 (15) [M + 2H]⁻, 699.1 (20) [M + H + Na]⁻. HR-MS (ESI⁻) for $C_{23}H_{21}O_{15}N_2FP_3$: [M + 2H]⁻ calculated 677.0144, found 677.0147.

7-Deaza-7-[4″-(benzo[*d*]oxazol-2‴-yl)-2″-fluorophenyl]-2′-deoxyadenosine 5′-*O*-Triphosphate (dA^{BOX}TP). dA^{BOX}TP was prepared according to the general procedure, **dA^{I}TP** (35.2 mg, 0.05 mmol), **2c** (38 mg, 0.075 mmol). The product was isolated as white solid (9 mg, 23%). ^1H NMR (499.8 MHz, D_2O, pD = 7.1, phosphate buffer): 2.42 (ddd, 1H, J_{gem} = 13.9, $J_{2'b,1'}$ = 5.7, $J_{2'b,3'}$ = 3.0, H-2′b); 2.61 (ddd, 1H, J_{gem} = 13.9, $J_{2'a,1'}$ = 8.4, $J_{2'a,3'}$ = 6.1, H-2′a); 4.06−4.16 (m, 2H, H-5′); 4.21 (m, 1H, H-4′); 4.71 (m, 1H, H-3′); 6.37 (dd, 1H, $J_{1',2'}$ = 8.4, 5.7, H-1′); 7.23 (t, 1H, $J_{5,4}$ = $J_{5,6}$ = 7.3, H-5-benzoxazole); 7.27 (t, 1H, $J_{6,5}$ = $J_{6,7}$ = 7.3, H-6-benzoxazole); 7.41 (m, 3H, H-6-C_6H_3F, H-4,7-benzoxazole); 7.49 (s, 1H, H-6-deazapurine); 7.77 (d, 1H, $J_{H,F}$ = 11.5, H-3-C_6H_3F); 7.79 (dd, 1H, $J_{5,6}$ = 9.1, H-5-C_6H_3F); 8.01 (s, 1H, H-2-deazapurine). ^{13}C NMR (125.7 MHz, D_2O, pD = 7.1, phosphate buffer): 41.0 (CH_2-2′); 68.3 (d, $J_{C,P}$ = 6.2, CH_2-5′); 73.8 (CH-3′); 85.5 (CH-1′); 87.8 (d, $J_{C,P}$ = 8.5, CH-4′); 103.7 (C-4a-deazapurine); 112.2 (C-5-deazapurine); 113.4 (CH-7-benzoxazole); 117.6 (d, $J_{C,F}$ = 25.8, CH-3-C_6H_3F); 121.4 (CH-4-benzoxazole); 125.1 (CH-6-deazapurine); 126.3 (CH-5-C_6H_3F); 127.2 (d, $J_{C,F}$ = 14.9, C-1-C_6H_3F); 127.7 (CH-5-benzoxazole); 128.6 (CH-6-benzoxazole); 129.0 (d, $J_{C,F}$ = 8.6, C-4-C_6H_3F); 134.7 (d, $J_{C,F}$ = 2.2, CH-6-C_6H_3F); 142.6 (C-3a-benzoxazole); 152.1 (C-7a-deazapurine); 152.6 (C-7a-benzoxazole); 153.6 (CH-2-deazapurine); 159.2 (C-4-deazapurine); 161.7 (d, $J_{C,F}$ = 246.0, C-2-C_6H_3F); 164.1 (d, $J_{C,F}$ = 2.7, C-2-benzoxazole). $^{31}P\{^1H\}$ NMR (202.3 MHz, D_2O, pD = 7.1, phosphate buffer): −21.28 (bdd, *J* = 19.4, 18.7, P_β); −10.49 (d, *J* = 18.7, P_α); −6.52 (bd, *J* = 19.4, P_γ). $^{19}F\{^1H\}$ NMR (470.3 MHz, D_2O, pD = 7.1, phosphate buffer): −110.5. MS (ESI⁻): *m*/*z* (%) 620.1 (100) [M + 2H - PO_3H]⁻, 642.1 (35) [M + H + Na - PO_3H]⁻ 700.0 (12) [M + 2H]⁻, 722.0 (16) [M + H + Na]⁻. HR-MS (ESI⁻) for $C_{24}H_{22}O_{13}N_5FP_3$: [M + 2H]⁻ calculated 700.0416, found 700.0396.

5-[4″-(Benzo[*d*]oxazol-2‴-yl)-2″-fluorophenyl]-2′-deoxyuridine 5′-*O*-Triphosphate (dU^{BOX}TP). dU^{BOX}TP was prepared according to the general procedure, **dU^{I}TP** (34 mg, 0.05 mmol), **2c** (38 mg, 0.075 mmol). The product was isolated as white solid (7.6 mg, 20%). ^1H NMR (499.8 MHz, D_2O, pD = 7.1, phosphate buffer): 2.45 (dd, 2H, $J_{2',1'}$ = 6.8, $J_{2',3'}$ = 5.1, H-2′); 4.14−4.25 (m, 3H, H-4′,5′); 4.66 (td, 1H, $J_{3',2'}$ = 5.1, $J_{3',4'}$ = 3.0, H-3′); 6.33 (t, 1H, $J_{1',2'}$ = 6.8, H-1′); 7.44 (td, 1H, $J_{5,4}$ = $J_{5,6}$ = 7.5, $J_{5,7}$ = 1.3, H-5-benzoxazole); 7.48 (td, 1H, $J_{6,5}$ = $J_{6,7}$ = 7.5, $J_{6,4}$ = 1.5, H-6-benzoxazole); 7.64 (dd, 1H, $J_{6,5}$ =8.0, $J_{H,F}$ = 7.6, H-6-C_6H_3F); 7.72 (ddd, 1H, $J_{7,6}$ = 7.5, $J_{7,5}$ = 1.3, $J_{7,4}$ = 0.7, H-7-benzoxazole); 7.75 (ddd, 1H, $J_{4,5}$ = 7.5, $J_{4,6}$ = 1.5, $J_{4,7}$ = 0.7, H-4-benzoxazole); 7.96 (dd, 1H, $J_{H,F}$ = 10.6, $J_{3,5}$ = 1.7, H-3-C_6H_3F); 8.01 (s, 1H, H-6); 8.05 (dd, 1H, $J_{5,6}$ = 8.0, $J_{5,3}$ = 1.7, H-5-C_6H_3F). ^{13}C NMR (125.7 MHz, D_2O, pD = 7.1, phosphate buffer): 41.3 (CH_2-2′); 68.0 (d, $J_{C,P}$ = 5.2, CH_2-5′); 70.4 (CH-3′); 88.4 (d, $J_{C,P}$ = 8.6, CH-4′); 88.6 (CH-1′); 112.6 (C-5); 113.9 (CH-7-benzoxazole); 117.3 (d, $J_{C,F}$ = 25.4, CH-3-C_6H_3F); 121.9 (CH-4-benzoxazole); 126.0 (d, $J_{C,F}$ = 15.4, C-1-C_6H_3F); 126.3 (d, $J_{C,F}$ = 3.0, CH-5-C_6H_3F); 127.9 (CH-5-benzoxazole); 128.9 (CH-6-benzoxazole); 130.8 (d, $J_{C,F}$ = 8.8, C-4-C_6H_3F); 135.4 (d, $J_{C,F}$ = 2.7, CH-6-C_6H_3F); 143.2 (C-3a-benzoxazole); 143.8 (CH-6); 153.1 (C-7a-benzoxazole); 154.0 (C-2); 162.8 (d, $J_{C,F}$ = 247.9, C-2-C_6H_3F); 164.9 (C-2-benzoxazole); 166.7 (C-4). $^{31}P\{^1H\}$ NMR (202.3 MHz, D_2O, pD = 7.1, phosphate buffer, ref(phosphate buffer) = 2.35 ppm): −21.41 (bt, *J* = 19.2, P_β); −10.66 (d, *J* = 19.2, P_α); −6.69 (bs, P_γ). $^{19}F\{^1H\}$ NMR (470.3 MHz, pD = 7.1, phosphate buffer): −109.0. MS (ESI⁻): *m*/*z* (%) 517.9 (90) [M + 2H - $2PO_3H$]⁻, 597.9 (65) [M + 2H - PO_3H]⁻, 619.9 (25) [M + H + Na - PO_3H]⁻, 678.0 (2) [M + 2H]⁻, 699.8 (13) [M + H + Na]⁻. HR-MS (ESI⁻) for $C_{22}H_{20}O_{15}N_3FP_3$: [M + 2H]⁻ calculated 678.0097, found 678.0098.

7-Deaza-7-[4″-(5‴-aminobenzo[*d*]oxazol-2‴-yl)-2″-fluorophenyl]-2′-deoxyadenosine 5′-*O*-Triphosphate (dA^{ABOX}TP). dA^{ABOX}TP was prepared according to the general procedure, **dA^{I}TP** (35.2 mg, 0.05 mmol), **2d** (50 mg, 0.075 mmol). The product was isolated as yellow solid (10.4 mg, 26%). ^1H NMR (499.8 MHz, D_2O,

dx.doi.org/10.1021/jo202321g | J. Org. Chem. 2012, 77, 1026−1044

pD = 7.1, phosphate buffer): 2.37 (ddd, 1H, J_{gem} = 13.8, $J_{2'b,1'}$ = 6.0, $J_{2'b,3'}$ = 2.9, H-2'b); 2.53 (ddd, 1H, J_{gem} = 13.8, $J_{2'a,1'}$ = 8.1, $J_{2'a,3'}$ = 6.4, H-2'a); 4.08 (dt, 1H, J_{gem} = 11.4, $J_{H,P}$ = $J_{5'b,4'}$ = 5.4, H-5'b); 4.13 (ddd, 1H, J_{gem} = 11.4, $J_{H,P}$ = 6.8, $J_{5'a,4'}$ = 4.7, H-5'a); 4.21 (ddd, 1H, $J_{4',5'}$ = 5.4, 4.7, $J_{4',3'}$ = 2.2, H-4'); 4.67 (ddd, 1H, $J_{3',2'}$ = 6.4, 2.9, $J_{3',4'}$ = 2.2, H-3'); 6.34 (dd, 1H, $J_{1',2'}$ = 8.1, 6.0, H-1'); 6.67–6.75 (m, 2H, H-4,6-benzoxazole); 7.14 (d, 1H, $J_{7,6}$ = 9.0, H-7-benzoxazole); 7.33 (t, 1H, $J_{6,5}$ = $J_{H,F}$ = 8.0, H-6-C_6H_3F); 7.42 (s, 1H, H-6-deazapurine); 7.64 (d, 1H, $J_{H,F}$ = 11.5, H-3-C_6H_3F); 7.67 (d, 1H, $J_{5,6}$ = 8.0, H-5-C_6H_3F); 8.05 (s, 1H, H-2-deazapurine). ^{13}C NMR (125.7 MHz, D_2O, pD = 7.1, phosphate buffer): 41.0 (CH_2-2'); 68.3 (CH_2-5'); 73.8 (CH-3'); 85.6 (CH-1'); 87.7 (d, $J_{C,P}$ = 7.9, CH-4'); 103.6 (C-4a-deazapurine); 107.6 (CH-4-benzoxazole); 112.2 (C-5-deazapurine); 113.5 (CH-7-benzoxazole); 117.3 (d, $J_{C,F}$ = 24.5, CH-3-C_6H_3F); 118.3 (CH-6-bezoxazole); 125.2 (CH-6-deazapurine); 126.1 (CH-5-C_6H_3F); 128.9 (d, $J_{C,F}$ = 15.2, C-1-C_6H_3F); 129.00 (d, $J_{C,F}$ = 6.5, C-4-C_6H_3F); 134.5 (CH-6-C_6H_3F); 143.5 (C-3a-benzoxazole); 146.0 (C-5-benzoxazole); 147.1 (C-7a-benzoxazole); 152.0 (C-7a-deazapurine); 153.2 (CH-2-deazapurine); 158.9 (C-4-deazapurine); 161.6 (d, $J_{C,F}$ = 243.7, C-2-C_6H_3F); 164.3 (C-2-benzoxazole). $^{31}P\{^1H\}$ NMR (202.3 MHz, D_2O, pD = 7.1, phosphate buffer, ref(phosphate buffer) = 2.35 ppm): −21.14 (t, J = 19.3, P_β); −10.15 (d, J = 19.3, P_α); −6.72 (bd, J = 19.3, P_γ). $^{19}F\{^1H\}$ NMR (470.3 MHz, D_2O, pD = 7.1, phosphate buffer): −110.7. MS (ESI$^-$): m/z (%) 635.2 (20) [M + 2H - PO_3H]$^-$, 657.2 (8) [M + H + Na - PO_3H]$^-$ 715.2 (3) [M + 2H]$^-$, 737.2 (6) [M + H + Na]$^-$. HR-MS (ESI$^-$) for $C_{24}H_{23}O_{13}N_6FP_3$: [M + 2H]$^-$ calculated 715.0525, found 715.0520.

5-[4″-(5‴-Aminobenzo[*d*]oxazol-2‴-yl)-2″-fluorophenyl]-2′-deoxyuridine 5′-*O*-Triphosphate (dU^{ABOX}TP). **dU^{ABOX}TP** was prepared according to the general procedure, **dU^{I}TP** (34 mg, 0.05 mmol), **2d** (50 mg, 0.075 mmol). The product was isolated as yellow solid (9.7 mg, 25%). ^{1}H NMR (499.8 MHz, D_2O, pD = 7.1, phosphate buffer): 2.44 (m, 2H, H-2'); 4.13–4.26 (m, 3H, H-4',5'); 4.65 (m, 1H, H-3'); 6.30 (t, 1H, $J_{1',2'}$ = 6.9, H-1'); 6.89 (dd, 1H, $J_{6,7}$ = 8.7, $J_{6,4}$ = 1.6, H-6-benzoxazole); 7.03 (s, 1H, H-4-benzoxazole); 7.46 (d, 1H, $J_{7,6}$ = 8.7, H-7-benzoxazole); 7.59 (dd, 1H, $J_{6,5}$ = 8.0, $J_{H,F}$ = 7.6, H-6-C_6H_3F); 7.82 (d, 1H, $J_{H,F}$ = 10.6, H-3-C_6H_3F); 7.95 (d, 1H, $J_{5,6}$ = 8.0, H-5-C_6H_3F); 7.97 (s, 1H, H-6). ^{13}C NMR (125.7 MHz, D_2O, pD = 7.1, phosphate buffer): 41.4 (CH_2-2'); 68.0 (d, $J_{C,P}$ = 5.6, CH_2-5'); 73.5 (CH-3'); 88.5 (d, $J_{C,P}$ = 8.6, CH-4'); 88.7 (CH-1'); 107.9 (CH-4-benzoxazole); 112.5 (C-5); 114.0 (CH-7-benzoxazole); 117.0 (d, $J_{C,F}$ = 24.9, CH-3-C_6H_3F); 118.5 (CH-6-bezoxazole); 125.7 (d, $J_{C,F}$ = 15.1, C-1-C_6H_3F); 126.1 (d, $J_{C,F}$ = 3.1, CH-5-C_6H_3F); 130.8 (d, $J_{C,F}$ = 9.0, C-4-C_6H_3F); 135.2 (d, $J_{C,F}$ = 3.2, CH-6-C_6H_3F); 143.7 (CH-6); 144.0 (C-3a-benzoxazole); 146.5 (C-7a-benzoxazole); 147.6 (C-5-benzoxazole); 153.9 (C-2); 162.7 (d, $J_{C,F}$ = 248.3, C-2-C_6H_3F); 165.1 (C-2-benzoxazole); 166.6 (C-4). $^{31}P\{^1H\}$ NMR (202.3 MHz, D_2O, pD = 7.1, phosphate buffer, ref(phosphate buffer) = 2.35 ppm): −21.40 (t, J = 19.5, P_β); −10.67 (d, J = 19.5, P_α); −6.67 (d, J = 19.5, P_γ). $^{19}F\{^1H\}$ NMR (470.3 MHz, D_2O, pD = 7.1, phosphate buffer): −108.9. MS (ESI$^-$): m/z (%) 612.9 (85) [M + 2H − PO_3H]$^-$, 634.9 (60) [M + H + Na - PO_3H]$^-$, 693.1 (8) [M + 2H]$^-$, 714.8 (30) [M + H + Na]$^-$. HR-MS (ESI$^-$) for $C_{22}H_{21}O_{15}N_4FP_3$: [M + 2H]$^-$ calculated 693.0206, found 693.0210.

Biochemical Materials. Synthetic ONs were purchased from Sigma-Aldrich (USA); for their sequences, see Table 1. Dynabeads M-280 streptavidin (DBStv) were obtained from Sigma-Aldrich (USA); Pwo DNA polymerase from PEQLAB (Germany); Vent (exo-) DNA polymerase, Klenow (exo-) fragment, and T4 polynucleotide kinase from New England Biolabs (Great Britain); DyNAzyme II DNA polymerace from Finnzymes (Finland); standard nucleoside triphosphates (dATP, dTTP, dCTP, and dGTP) from Sigma-Aldrich; and γ-^{32}P-ATP from MP Empowered Discovery (USA). Other chemicals were of analytical grade.

Primer Extension. Primer extension for analysis by polyacrylamide gel electrophoresis: The reaction mixture contained primer (0.15 μM) template (0.22 μM), natural dNTPs (200 μM), dN^{R}TPs, buffer, and DNA polymerase (0.1 U). The reaction mixture was incubated for 15 min (30 min for 4 modified ONs) at 60 °C and analyzed by polyacrylamide gel electrophoresis. Primers were ^{32}P-prelabeled at 5′-end allowing radiographic detection. Preparative primer extension for fluorescence and NMR studies: Reaction mixture for oligonucleotide preparation contained primer (6.6 μM), 5′-biotinylated template (6.6 μM), dNTPs (200 μM), dN^{R}TPs (200 μM), 10x buffer, and KOD XL DNA polymerase (7.5 U). Reaction was incubated for 1 h. Biotinylated templates were used allowing magnetoseparation.

Isolation of Single-Strand Oligonucleotides by Magneto-separatic Procedure. The reaction mixture containing 0.3 M NaCl was added to a suspension of magnetic beads (50 μL of the MagPrep P-25 Streptavidin Particles stock solution from Novagen) washed three times by 450 μL of buffer (0.3 M NaCl, 10 mM TRIS, pH = 7.4). The suspension was shaken for 40 min at room temperature, allowing the oligonucleotides to bind to the Magselect beads, which were washed three times by 500 μL of PBS solution (0.14 M NaCl, 3 mM KCl, 4 mM sodium phosphate pH = 7.4), three times by 500 μL of buffer (0.3 M NaCl, 10 mM TRIS, pH = 7.4). Single-strand oligonucleotides were released by shaking and heating of the sample to 75 °C for 2 min. Each medium exchange was performed using a magnetoseparator (Dynal, Norway). The samples were desalted by Amicon Ultra centrifugal filters containing 3K cellulose membrane and lyophilized.

Characterization of Oligonucleotides. Oligonucleotides were characterized by MALDI-TOF mass spectrometry. A mixture of 3-hydroxypicolinic acid (HPA)/picolinic acid (PA)/ammonium tartrate in the ratio 8/1/1 in 50% acetonitrile was used as matrix for MALDI-TOF measurement. Then 2 μL of the matrix and 1 μL of the sample were mixed on MTP 384 polished steel target by use of anchor-chip desk. The acceleration tension in reflectron mode was 19.5 kV and range of measurement 3–13 kDa.

Table 7

ON1 (A^{BIF}) [M + H]$^+$	calcd	6172.1	found	6174.5
ON1 (A^{BFU}) [M + H]$^+$	calcd	6182.1	found	6183.9
ON1 (A^{BOX}) [M + H]$^+$	calcd	6185.1	found	6185.7
ON1 (A^{ABOX}) [M + H]$^+$	calcd	6200.1	found	6201.1
ON2 (U^{BFU}) [M + H]$^+$	calcd	6160.1	found	6161.7
ON2 (U^{BOX}) [M + H]$^+$	calcd	6161.1	found	6162.8
ON2 (U^{ABOX}) [M + H]$^+$	calcd	6176.1	found	6177.4
ON3 (U^{BFU}) [M + H]$^+$	calcd	9990.7	found	9996.0
ON3 (U^{BOX}) [M + H]$^+$	calcd	9991.7	found	9996.7
ON3 (U^{ABOX}) [M + H]$^+$	calcd	10006.7	found	10010.9
ON5 (U^{BFU}) [M + H]$^+$	calcd	7825.7	found	7826.7
ON5 (U^{BOX}) [M + H]$^+$	calcd	7826.7	found	7827.4
ON5 (U^{ABOX}) [M + H]$^+$	calcd	7841.7	found	7842.8
ON6 (U^{BFU}) [M + H]$^+$	calcd	9539.6	found	9545.7
ON6 (U^{BOX}) [M + H]$^+$	calcd	9540.7	found	9543.9
ON6 (U^{ABOX}) [M + H]$^+$	calcd	9555.6	found	9558.3
ON17 (A^{BFU}) [M + H]$^+$	calcd	10449.8	found	10452.1
ON17 (A^{BOX}) [M + H]$^+$	calcd	10453.8	found	10454.1
ON17 (U^{BOX}) [M + H]$^+$	calcd	10399.2	found	10404.8

Fluorescence Measurements. Samples were dissolved in pH adjusted 20 mM buffers. Citric buffer was used for the range of pH = 3–5, phosphate buffer for pH = 5.25–7.75, and borate buffer for pH = 8–10. All fluorescence measurements of DNA were performed in solution of phosphate buffer adjusted to pH = 6.

The fluorescence measurements were performed on a spectrofluorometer with 220–850 nm range, xenon source, excitation and emission wavelength scans, spectral bandwidth 1–16 nm, PMT detector, scan rate 3–6000 nm/min, and Saya-Namioka grating monochromator. We used the comparative method for recording fluorescence quantum yield of a sample using a 10 mM solution of quinine sulfate in 0.1 M H_2SO_4 (in H_2O) as a standard (Φ = 0.54). The area of the emission spectrum was integrated using the instrumentation software, and the quantum yield was calculated according to the following equation:

$$\Phi_{F(SA)} = \Phi_{F(ST)}[F_{(SA)}/F_{(ST)}][A_{(ST)}/A_{(SA)}][n_{(SA)}/n_{(ST)}]^2$$

dx.doi.org/10.1021/jo202321g | J. Org. Chem. 2012, 77, 1026–1044

Here, $\Phi_{F(SA)}$ and $\Phi_{F(ST)}$ are the fluorescence quantum yields of the sample and the standard, respectively. The terms $F_{(SA)}$ and $F_{(ST)}$ are the integrated fluorescence intensities of the sample and the standard, respectively; $A_{(SA)}$ and $A_{(ST)}$ are the optical densities of the sample and the standard solution at the wavelength of excitation, respectively; and $n_{(SA)}$ and $n_{(ST)}$ are the values of the refractive index for the solvents used for the sample, respectively.

^{19}F NMR Measurements. $^{19}F\{^1H\}$ NMR spectra were recorded on a 500 MHz spectrometer in D_2O solutions containing 10 mM phosphate buffer (pD = 7.1) and 0.1 mM EDTA. Typical experimental parameters for measurements of oligonucleotides were chosen as follows: 38 k data points (spectral width 40 ppm, transmitter frequency offset −110 ppm), 25 k scans, acquisition time 1 s and relaxation delay 1 s. All time domain data were processed with an exponential window function using a line broadening factor of 10 Hz for single-stranded DNA containing hairpin and 2 or 5 Hz for duplex.

COMPUTATIONAL DETAILS

Quantum chemical calculations were carried out using Turbomole 6.3[24] and Gaussian 09[25] program packages. All results reported in the manuscript were obtained using the medium-sized def2-SVP basis set.[26] Accurate gas-phase absorption and emission spectra were obtained using the RI-CC2 method, which was also used for the optimization of the S_1 state in order to obtain S_1 minimum from which the emission to the ground S_0 state (in the geometry of the S_1 minimum) was calculated. In order to address the effect of solvation, the SMD model[27] available in Gaussian 09 together with the long-range corrected version of the standard and widely used B3LYP functional (Coulomb-attenuated method), CAM-B3LY,P[28] was used to avoid severe underestimation of the charge-tranfer excitations by B3LYP (and other standard functionals). We have used two solvents representing less polar (1,4-dioxane; ε_r = 2.2099) and polar (acetonitrile; ε_r = 35.688) moieties.

The vertical absorption spectra in the solvent were calculated using state-specific (S_1) nonequilibrium solvation with the solvent reaction field corresponding to the ground state. The emission spectra were calculated using (i) TD-DFT (CAM-B3LYP) optimization of the S_1 state and linear response, equilibrium solvation (of the S_1 state) and (ii) vertical emission to the ground state (at the S_1 geometry) subtracting energy of the S_1 excited state using the state-specific equilibrium solvation from the energy of the S_0 state using nonequilibrium solvation (i.e., the solvent reaction field corresponding to the S_1 state). This represents the recommended protocol for the conceptually rigorous absorption and emission energies in solvent.[29]

ASSOCIATED CONTENT

Supporting Information

Additional figures of PEX, quantification of solvatochromic effects, fluorescence and ^{19}F NMR spectra, copies of all NMR spectra. This material is available free of charge via the Internet at http://pubs.acs.org.

AUTHOR INFORMATION

Corresponding Author

*E-mail: hocek@uochb.cas.cz.

ACKNOWLEDGMENTS

This work is a part of the research projects Z4 055 0506 supported by the Academy of Sciences of the Czech Republic. It was specifically supported by the Czech Science Foundation (203/09/0317) and by Gilead Sciences, Inc. (Foster City, CA, USA). The authors thank Dr. Dana Nachtigallová for helpful discussions.

REFERENCES

(1) (a) Lavis, L. D.; Raines, R. T. *ACS Chem. Biol.* **2008**, *3*, 142−155. (b) J. N. Wilson, J. N.; Kool, E. T. *Org. Biomol. Chem.* **2006**, *4*, 4265−4274.

(2) (a) Smith, L. M.; Sanders, J. Z.; Kaiser, R. J.; Hughes, P.; Dodd, C.; Connell, C. R.; Heiner, C.; Kent, S. B. H.; Hood, L. E. *Nature* **1986**, *321*, 674−679. (b) Guo, J.; Xu, N.; Li, Z.; Zhang, S.; Wu, J.; Kim, D. H.; Marma, M. S.; Meng, Q.; Cao, H.; Li, X.; Shi, S.; Yu, L.; Kalachikov, S.; Russo, J. J.; Turro, N. J.; Ju, J. *Proc. Natl. Acad. Sci. U.S.A.* **2008**, *105*, 9145−9150.

(3) Tyagi, S.; Kramer, F. R. *Nat. Biotechnol.* **1996**, *14*, 303−308.

(4) (a) Greco, N. J.; Tor, Y. *Tetrahedron* **2007**, *63*, 3515−3527. (b) Greco, N. J.; Tor, Y. *J. Am. Chem. Soc.* **2005**, *127*, 10784−10785. (c) Srivatsan, S. G.; Tor, Y. *J. Am. Chem. Soc.* **2007**, *129*, 2044−2053. (d) Pawar, M. G.; Srivatsan, S. G. *Org. Lett.* **2011**, *13*, 1114−1117. (e) Greco, N. J.; Sinkeldam, R. W.; Tor, Y. *Org. Lett.* **2009**, *11*, 1115−1118. (f) Wanninger-Weiss, C.; Valis, L.; Wagenknecht, H.-A. *Bioorg. Med. Chem.* **2008**, *16*, 100−106.

(5) (a) Hudson, R. H. E.; Ghorbani-Choghamarani, A. *Org. Biomol. Chem.* **2007**, *5*, 1845−1848. (b) Capobianco, M. L.; Cazzato, A.; Alesi, S.; Barbarella, G. *Bioconjugate Chem.* **2008**, *19*, 171−177. (c) Ryu, J. H.; Seo, Y. J.; Hwang, G. T.; Lee, J. Y.; Kim, B. H. *Tetrahedron* **2007**, *63*, 3538−3547. (d) Xiao, Q.; Ranasinghe, R. T.; Tang, A. M. P.; Brown, T. *Tetrahedron* **2007**, *63*, 3483−3490. (e) Sessler, J. L; Sathiosatham, M.; Brown, C. T.; Rhodes, T. A.; Wiederrecht, G. *J. Am. Chem. Soc.* **2001**, *123*, 3655−3660. (f) Skorobogatyi, M. V.; Malakov, A. D.; Pchelintseva, A. A.; Turban, A. A.; Bondarev, S. L.; Korshun, V. A. *ChemBioChem* **2006**, *7*, 810−816.

(6) (a) Okamoto, A.; Tainaka, K.; Saito, I. *J. Am. Chem. Soc.* **2003**, *125*, 4972−4973. (b) Okamoto, A.; Tanaka, K.; Fukuta, T.; Saito, I. *J. Am. Chem. Soc.* **2003**, *125*, 9296−9297. (c) Gardarson, H.; Kale, A.; Sigurdsson, S. T. *ChemBioChem* **2011**, *12*, 567−575. (d) Cekan, P; Sigurdsson, S. T. *Chem. Commun.* **2008**, *29*, 3393−3395. (e) Xie, Y.; Maxson, T.; Tor, Y. *Org. Biomol. Chem.* **2010**, *8*, 5053−5055. (f) Srivatsan, S. G.; Weizman, H.; Tor, Y. *Org. Biomol. Chem.* **2008**, *6*, 1334−1338. (g) Datta, K.; Johnson, N. P.; Villani, G.; Marcus, A. H.; von Hippel, P. H. *Nucleic Acids Res.* **2011**, E-pub ahead of print, DOI: 10.1093/nar/gkr858.

(7) (a) Karunakaran, V.; Perez Lustres, J. L.; Zhao, L.; Ernsting, N. P.; Seitz, O. *J. Am. Chem. Soc.* **2006**, *128*, 2954−2962. (b) Kummer, S.; Knoll, A.; Socher, E.; Bethge, L.; Herrmann, A.; Seitz, O. *Angew. Chem., Int. Ed.* **2011**, *50*, 1931−1934. (c) Holzhauser, C.; Berndl, S.; Menacher, F.; Breunig, M.; Göpferich, A.; Wagenknecht, H.-A. *Eur. J. Org. Chem.* **2010**, *7*, 1239−1248. (d) Berndl, S.; Wagenknecht, H.-A. *Angew. Chem., Int. Ed.* **2009**, *48*, 2418−2421. (e) Asanuma, H.; Kashida, H.; Liang, X.; Komiyama, M. *Chem. Commun.* **2003**, *7*, 1536−1537. (f) Coleman, R. S.; Berg, M. A.; Murphy, C. J. *Tetrahedron* **2007**, *63*, 3450−3456.

(8) (a) Okamoto, A.; Kanatani, K.; Saito, I. *J. Am. Chem. Soc.* **2004**, *126*, 4820−4827. (b) Tainaka, K.; Tanaka, K.; Ikeda, S.; Nishiza, K.-I.; Unzai, T.; Fujiwara, Y.; Saito, I.; Okamoto, A. *J. Am. Chem. Soc.* **2007**, *129*, 4776−4784. (c) Saito, Y.; Motegi, K.; Bag, S. S.; Saito, I. *Bioorg. Med. Chem.* **2008**, *16*, 107−113.

(9) (a) Han, J.; Burgess, K. *Chem. Rev.* **2010**, *110*, 2709−2728. (b) Craig, I. M.; Duong, H. M.; Wudl, F.; Schwartz, B. J. *Chem. Phys. Lett.* **2009**, *477*, 319−324.

(10) Hanson, G. T.; McAnaney, T. B.; Park, E. S.; Rendell, M. E. P.; Yarbrough, D. K.; Chu, S.; Xi, L.; Boxer, S. G.; Montrose, M. H.; Remington, S. J. *Biochemistry* **2002**, *41*, 15477−15488.

(11) Sun, K. M.; McLaughlin, C. K.; Lantero, D. R.; Manderville, R. A. *J. Am. Chem. Soc.* **2007**, *129*, 1894−1895.

(12) (a) Barhate, N. B.; Barhate, R. N.; Cekan, P.; Drobny, G.; Sigurdsson, S. T. *Org. Lett.* **2008**, *10*, 2745−2747. (b) Puffer, B.; Kreutz, C.; Rieder, U.; Bert, M.-O.; Konrat, R.; Micura, R. *Nucleic Acids Res.* **2009**, *37*, 7728−7740. (c) Kreutz, C.; Kahlig, H.; Konrat, R.; Micura, R. *Angew. Chem., Int. Ed.* **2006**, *45*, 3450−3453. (d) Graber, D.; Moroder, H.; Micura, R. *J. Am. Chem. Soc.* **2008**, *130*, 17230−17231.

(13) Reviews: (a) Hocek, M.; Fojta, M. *Org. Biomol. Chem.* **2008**, *6*, 2233−2241. (b) Weisbrod, S. H.; Marx, A. *Chem. Commun.* **2007**, 1828−1830.

(14) (a) Thoresen, L. H.; Jiao, G.-S.; Haaland, W. C.; Metzker, M. L.; Burgess, K. *Chem.—Eur. J.* **2003**, *9*, 4603−4610. (b) Shoji, A.;

Hasegawa, T.; Kuwahara, M.; Ozaki, H.; Sawai, H. *Bioorg. Med. Chem. Lett.* **2007**, *17*, 776−779.
(15) (a) Brázdilová, P.; Vrábel, M.; Pohl, R.; Pivoňková, H.; Havran, L.; Hocek, M.; Fojta, M. *Chem.—Eur. J.* **2007**, *13*, 9527−9533. (b) Cahová, H.; Havran, L.; Brázdilová, P.; Pivoňková, H.; Pohl, R.; Fojta, M.; Hocek, M. *Angew. Chem., Int. Ed.* **2008**, *47*, 2059−2062. (c) Vrábel, M.; Horáková, P.; Pivoňková, H.; Kalachova, L.; Černocká, H.; Cahová, H.; Pohl, R.; Šebest, P.; Havran, L.; Hocek, M.; Fojta, M. *Chem.—Eur. J.* **2009**, *15*, 1144−1154. (d) Macíčková-Cahová, H.; Pohl, R.; Horáková, P.; Havran, L.; Špaček, J.; Fojta, M.; Hocek, M. *Chem.—Eur. J.* **2011**, *17*, 5833−5841.
(16) Obeid, S.; Yulikow, M.; Jeschke, G.; Marx, A. *Angew. Chem., Int. Ed.* **2008**, *47*, 6782−6785.
(17) Srivatsan, S. G.; Tor, Y. *Chem. Asian J.* **2009**, *4*, 419−427.
(18) Strobel, S. A.; Jones, F. D.; Oyelere, A. K.; Ryder, S. P. *Nucleic Acids Res. Suppl.* **2003**, *3*, 229−230.
(19) pK_a data compiled by R. Williams: http://research.chem.psu.edu/brpgroup/pKa_compilation.pdf.
(20) Seidel, C. A. M.; Schulz, A.; Sauer, M. H. M. *J. Phys. Chem.* **1996**, *100*, 5541−5553.
(21) Dierckx, A.; Dinér, P.; El-Sagheer, A. H.; Kumar1, J. D.; Brown, T.; Grøtli, M.; Wilhelmsson, L. M. *Nucleic Acids Res.* **2011**, *39*, 4513−4524.
(22) Dohno, C.; Saito, I. *Nucleic Acids Symp. Ser.* **2004**, *48*, 93−94.
(23) van Dongen, M. J. P.; Mooren, M. M. W.; Willems, E. F. A.; van der Marel, G. A.; van Boom, J. H.; Wijmenga, S. S.; Hilbers, C. W. *Nucleic Acids Res.* **1997**, *25*, 1537−1547.
(24) Treutler, O.; Ahlrichs, R. *J. Chem. Phys.* **1995**, *102*, 346−354.
(25) Frisch, M. J.; Trucks, G. W.; Schlegel, H. B.; Scuseria, G. E.; Robb, M. A.; Cheeseman, J. R.; Scalmani, G.; Barone, V.; Mennucci, B.; Petersson, G. A.; Nakatsuji, H.; Caricato, M.; Li, X.; Hratchian, H. P.; Izmaylov, A. F.; Bloino, J.; Zheng, G.; Sonnenberg, J. L.; Hada, M.; Ehara, M.; Toyota, K.; Fukuda, R.; Hasegawa, J.; Ishida, M.; Nakajima, T.; Honda, Y.; Kitao, O.; Nakai, H.; Vreven, T.; Montgomery, Jr., J. A.; Peralta, J. E.; Ogliaro, F.; Bearpark, M.; Heyd, J. J.; Brothers, E.; Kudin, K. N.; Staroverov, V. N.; Kobayashi, R.; Normand, J.; Raghavachari, K.; Rendell, A.; Burant, J. C.; Iyengar, S. S.; Tomasi, J.; Cossi, M.; Rega, N.; Millam, N. J.; Klene, M.; Knox, J. E.; Cross, J. B.; Bakken, V.; Adamo, C.; Jaramillo, J.; Gomperts, R.; Stratmann, R. E.; Yazyev, O.; Austin, A. J.; Cammi, R.; Pomelli, C.; Ochterski, J. W.; Martin, R. L.; Morokuma, K.; Zakrzewski, V. G.; Voth, G. A.; Salvador, P.; Dannenberg, J. J.; Dapprich, S.; Daniels, A. D.; Farkas, Ö.; Foresman, J. B.; Ortiz, J. V.; Cioslowski, J.; Fox, D. J. *Gaussian 09*, Revision A.02; Gaussian, Inc.: Wallingford CT, 2009.
(26) Weigend, F.; Ahlrichs, R. *Phys. Chem. Chem. Phys.* **2005**, *7*, 3297−3305.
(27) Marenich, A. V.; Cramer, C. J.; Truhlar, D. G. *J. Phys. Chem. B* **2009**, *113*, 6378−6396.
(28) Yanai, T.; Tew, D; Handy, N. *Chem. Phys. Lett.* **2004**, *393*, 51−57.
(29) http://www.gaussian.com/g_tech/g_ur/k_scrf.htm